Fraunhofer
ITWM

H. Lang, J. Linn, M. Arnold

Multibody dynamics simulation of geometrically exact Cosserat rods

Berichte des Fraunhofer ITWM, Nr. 209 (2011)

ISSN 1434-9973

Bericht 209 (2011)

Die Veröffentlichungen in der Berichtsreihe des Fraunhofer ITWM können bezogen werden über:

Fraunhofer-Institut für Techno- und
Wirtschaftsmathematik ITWM
Fraunhofer-Platz 1

67663 Kaiserslautern
Germany

Telefon: +49(0)631/3160 0-4674
Telefax: +49(0)631/3160 0-5674
E-Mail: presse@itwm.fraunhofer.de
Internet: www.itwm.fraunhofer.de

Vorwort

Das Tätigkeitsfeld des Fraunhofer-Instituts für Techno- und Wirtschaftsmathematik ITWM umfasst anwendungsnahe Grundlagenforschung, angewandte Forschung sowie Beratung und kundenspezifische Lösungen auf allen Gebieten, die für Techno- und Wirtschaftsmathematik bedeutsam sind.

In der Reihe »Berichte des Fraunhofer ITWM« soll die Arbeit des Instituts kontinuierlich einer interessierten Öffentlichkeit in Industrie, Wirtschaft und Wissenschaft vorgestellt werden. Durch die enge Verzahnung mit dem Fachbereich Mathematik der Universität Kaiserslautern sowie durch zahlreiche Kooperationen mit internationalen Institutionen und Hochschulen in den Bereichen Ausbildung und Forschung ist ein großes Potenzial für Forschungsberichte vorhanden. In die Berichtreihe werden sowohl hervorragende Diplom- und Projektarbeiten und Dissertationen als auch Forschungsberichte der Institutsmitarbeiter und Institutsgäste zu aktuellen Fragen der Techno- und Wirtschaftsmathematik aufgenommen.

Darüber hinaus bietet die Reihe ein Forum für die Berichterstattung über die zahlreichen Kooperationsprojekte des Instituts mit Partnern aus Industrie und Wirtschaft.

Berichterstattung heißt hier Dokumentation des Transfers aktueller Ergebnisse aus mathematischer Forschungs- und Entwicklungsarbeit in industrielle Anwendungen und Softwareprodukte – und umgekehrt, denn Probleme der Praxis generieren neue interessante mathematische Fragestellungen.

Prof. Dr. Dieter Prätzel-Wolters
Institutsleiter

Kaiserslautern, im Juni 2001

Multibody dynamics simulation of geometrically exact Cosserat rods

Holger Lang[♭], Joachim Linn[♭], Martin Arnold[♯]

[♭] Fraunhofer Institute for Industrial Mathematics
Fraunhofer Platz 1, 67663 Kaiserslautern, Germany
holger.lang@itwm.fraunhofer.de, *joachim.linn@itwm.fraunhofer.de*,

[♯] Institute for Mathematics, Martin-Luther-Universität Halle-Wittenberg
06099 Halle (Saale), Germany
martin.arnold@mathematik.uni-halle.de

Abstract

In this paper, we present a viscoelastic rod model that is suitable for fast and accurate dynamic simulations. It is based on Cosserat's geometrically exact theory of rods and is able to represent *extension, shearing* ('stiff' dof), *bending* and *torsion* ('soft' dof). For inner dissipation, a consistent damping potential proposed by Antman is chosen. We parametrise the rotational dof by unit quaternions and directly use the quaternionic evolution differential equation for the discretisation of the Cosserat rod curvature.

The discrete version of our rod model is obtained via a finite difference discretisation on a staggered grid. After an index reduction from three to zero, the right-hand side function f and the Jacobian $\partial f/\partial(q, v, t)$ of the dynamical system $\dot{q} = v$, $\dot{v} = f(q, v, t)$ is free of higher algebraic (e. g. root) or transcendental (e. g. trigonometric or exponential) functions and therefore cheap to evaluate. A comparison with Abaqus finite element results demonstrates the correct mechanical behaviour of our discrete rod model. For the time integration of the system, we use well established stiff solvers like Radau5 or Daspk. As our model yields computational times within milliseconds, it is suitable for interactive applications in 'virtual reality' as well as for multibody dynamics simulation.

Keywords. Flexible multibody dynamics, Large deformations, Finite rotations, Constrained mechanical systems, Structural dynamics.

1 Introduction

For rods — i. e. slender one dimensional flexible structures — the overall deformation as response to moderate external loads may become large, although locally the stresses and strains remain small. The *Cosserat rod model* [1, 3, 61, 62] is an appropriate model for the geometrically exact simulation of deformable rods in space (statics) or space-time (quasistatics or dynamics). A Cosserat rod can be considered as the geometrically nonlinear generalisation of a Timoshenko-Reissner beam. In contrast to a Kirchhoff rod, which can be considered as a geometrically nonlinear generalisation of an Euler-Bernoulli beam, a Cosserat rod allows to model not only bending and torsion — these are 'soft dof' —, but as well extension and shearing — these are 'stiff dof'.
This article is concerned with a discrete finite difference (FD) Cosserat rod model that is firmly based on structural mechanics and applicable to compute dynamical deformations of rods very fast and sufficiently accurate. We continue the work [40, 41] presented at Eccomas 2007, which considered the fast simulation of geometrically exact Kirchhoff rods in the quasistatic case, and complement recent investigations [33] of discrete FD type Cosserat rods within the framework of Discrete Lagrangian Mechanics.

The paper is structured as follows: In section 2, we describe the basic equations for a Cosserat rod in the continuum, where we formulate the rotational dof of the rod directly in terms of unit quaternions. Of course, other possibilities such as Rodriguez parameters, rotation vectors, Euler or Cardan angles, exist [6, 14, 24, 50, 56]. All of them have their pros and cons. So as a pro, gimbal locking can be avoided with quaternions. A con is that they must be kept at unity length.
In section 3, we present our discrete numerical model of the Cosserat rod, based on finite differences. In contrast to a displacement based discretisation by the finite element method (FEM), where the primary

unknowns are situated at the nodes (= vertices), we suggest a discretisation on a *staggered grid*. This means that the translatory resp. the rotatory dof are ordered in an alternating fashion and that the trapezoidal resp. midpoint quadrature formulas form the basis for the approximation of the internal energy integrals.
This construction allows to interpret the discrete Cosserat rod as a sequence of (almost) rigid cylinders with the primary rotatory dof situated at the cylinder centers of mass. Likewise, the discretised energy terms may be interpreted as bushings which connect the rigid body dof of adjacent cylinders by appropriate springs and dampers. Here the parameters of these 'springs' and 'dampers' are rigorously derived from the continuous Cosserat strain and curvature relations. Whereas the extensional and shearing strains, which belong to such cylinders, are discretised via finite differences in the one and only one canonical standard fashion, several choices for the discrete bending and torsion curvature measures are possible. These curvatures belong to the vertices between the cylinders and result from various possible rotation interpolations of varying accuracy and computational costs.
We formulate the final discrete model as a constrained mechanical system, resulting in the well known Lagrangian DAE system of index three. Index reduction to zero plus introduction of Baumgarte penalty accelerations yields a universal ODE formulation, suitable for any ODE solver. As an alternative to the Baumgarte method, stabilisation by projection is as well convenient and cheap. For our approach, the inverse mass-constraint matrix is explicitly known, and multiplication with the latter is exactly as expensive as multiplication with the mass-constraint matrix itself. The model can be implemented using algebraic expressions free of trigonometric and square root functions, which permits extremely cheap right hand side function and Jacobian evaluations. Moreover, both extensible and inextensible Kirchhoff rod models can be conveniently fed into this framework as well.
In section 4, we present accurate numerical results, compared to ABAQUS FE solutions. In view of applications in robotics and assembly simulation as well as interactive deformations of flexible 1D structures in virtual reality environments we are especially interested in moderately fast motions dominated rather by the internal forces and moments associated to bending and twisting than inertial effects. In such cases we propose to impose strong damping on extension and shearing, which are of subordinate importance, and to solve the resulting stiff system via well established methods [28, 29, 49]. As our model allows for accurate computations within milliseconds, it is likewise adequate for multibody dynamics simulations.

Where can this work be situated within the state of the art rod models?
The handling of flexible objects in **multibody dynamics** simulations has been a long term field of research until today [10, 11, 14, 54, 57, 58, 60]. The classical approach in industrial applications, which is supported by today's commercial software packages such as SIMPACK, ADAMS or VIRTUALLAB, represents flexible structures by vibrational modes, e. g. of Craig / Bampton type [18, 19], that are obtained from numerical modal analysis within the range of linear elasticity. Such methods are suitable and accurate to represent oscillatory response that results from *linear* response of the flexible structure.
Unlike that, our approach is not of modal kind, but based on a geometrically nonlinear structural model. However, our method of discretisation contrasts the usual one in computational continuum mechanics, where the **finite element** approach is favored [10, 11, 13, 14, 20, 31, 32, 61, 62] due to its general applicability for arbitrarily complex geometries. While the geometrical complexity of 2D and 3D domains often implies practical limitations for the applicability of the conceptually simple FD approach, this is not the case for the 1D domain of a rod model.
A general problem in geometrically nonlinear FE is the proper interpolation of the finite rotations [7, 20, 52] such that objectivity of the strain measures is maintained, i. e. invariance under rigid body motions. In multibody dynamics, this problem is successfully addressed by the absolute nodal coordinate formulation (ANCF) [57, 58].
However, especially FE of higher order require sophisticated and technically intricate interpolation procedures that lead to models with expensive right hand side functions and Jacobians. In contrast to these rather general approaches, the finite difference based method being presented below is tailored to nonlinear rod models resulting in a very straightforward solution scheme that maintains objectivity by construction.
Our approach is inspired by FD type discretisations of inextensible Kirchhoff rods using insights from *Discrete Differential Geometry* (DDG) [8, 12]. The comparison to physical experiments shown in [8]

demonstrate that such discretisation techniques yield a physically correct model behaviour even at very coarse discretisations. We refer to [33] for a brief discussion of the DDG aspects for a FD type discretisation of the strain measure of Cosserat rods and its relation to low order FE using piecewise linear shape functions.

2 Geometrically exact Cosserat rods in the continuum

Our starting point for the continuous Cosserat rod model is Simo's exposition [61, 62] of the model proposed earlier by Antman and Reissner [1, 51]. For the constitutive material behaviour, we choose a simple linear viscoelastic one [2, 3]. The elastic parameters can be straightforwardly deduced from material and geometric parameters [42]. Concerning the damping model, we note that it is macroscopic and phenomenological, it comprises not only pure material damping, but also miscellaneous damping mechanisms. We assume both the elastic and viscoelastic parts as diagonal. The generalisation to non-diagonal, symmetric and positively definite constitutive Hookean tensors or to nonlinear hyperelastic materials is straightforward. We concentrate on the description of the internal potential, dissipation and kinetic energies in sections 2.1, 2.2 and 2.3 respectively, as these will be the basis for the discrete model later. In section 2.4 we give a detailed exposition of the dynamic equations of motion with the rotatory part formulated in terms of quaternions.

We start with the **kinematics** for the Cosserat rod. The Cosserat rod is completely determined by its *centerline* of mass centroids

$$x : [0, L] \times [0, T] \to \mathbb{R}^3, \qquad (s, t) \mapsto x(s, t)$$

and its *unit quaternion field*

$$p : [0, L] \times [0, T] \to \mathbb{S}^3 = \partial B_1^{\mathbb{H}}(0) \hookrightarrow \mathbb{H}, \qquad (s, t) \mapsto p(s, t),$$

see also [21, 39]. For our purposes, the set of unit quaternions $\mathbb{S}^3 = \partial B_1^{\mathbb{H}}(0) = \{p \in \mathbb{H} : \|p\| = 1\} \subset \mathbb{H}$, which is a subgroup of the multiplicative quaternionic group $\mathbb{H}$, provides a convenient representation of — non-commutative — spatial rotations of orthonormal frames, which are elements of the group $SO(3) = \{Q \in \mathbb{R}^{3\times 3} : QQ^\top = Q^\top Q = I, \det Q = 1\}$. The quaternion field uniquely determines its *orthonormal frame field*

$$R \circ p : [0, L] \times [0, T] \xrightarrow{p} \mathbb{S}^3 = \partial B_1^{\mathbb{H}}(0) \xrightarrow{R} SO(3), \qquad (s, t) \mapsto R\big(p(s, t)\big).$$

The situation is depicted in Figure 1. Any point of the deformed rod in space s and time t is addressed by the map $[0, L] \times [0, T] \times \mathcal{A} \ni (s, t, (\xi_1, \xi_2)) \mapsto x(s, t) + \xi_1 d^1(p(s, t)) + \xi_2 d^2(p(s, t))$. The parameter $s \in [0, L]$ is the arc length of the undeformed rod centerline, where $L > 0$ is the total arc length of the undeformed centerline and $\mathcal{A} \subset \mathbb{R}^2$ is a bounded, connected coordinate domain for the coordinates (ξ_1, ξ_2) in the cross section, which is assumed to remain rigid and plane throughout the deformation. In classical differential geometry, the object $(x(\cdot, t), (R \circ p)(\cdot, t))$ constitutes a so-called 'framed curve'. For a quaternion $p = p_0 + \hat{p} = \Re(p) + \Im(p) = (p_0; p_1, p_2, p_3)^\top \in \mathbb{H}$ the frame $R(p)$ is given by the *Euler map*

$$R : \mathbb{H} \to \mathbb{R}SO(3), \qquad p \mapsto R(p) = \big(d^1(p) \,|\, d^2(p) \,|\, d^3(p)\big) = \big(2p_0^2 - \|p\|^2\big)\mathcal{I} + 2\hat{p} \otimes \hat{p} + 2p_0\mathcal{E}(\hat{p}) \qquad (1)$$

with the alternating skew tensor $\mathcal{E}$, which identifies skew tensors in $so(3)$ with their corresponding axial vectors in $\mathbb{R}^3$ via

$$\mathcal{E} : \mathbb{R}^3 = \Im(\mathbb{H}) \to so(3), \qquad \mathcal{E}(u) = \begin{pmatrix} 0 & -u_3 & u_2 \\ u_3 & 0 & -u_1 \\ -u_2 & u_1 & 0 \end{pmatrix}, \qquad \mathcal{E}(u)v = u \times v \quad \text{for } u, v \in \mathbb{R}^3.$$

We write $u \simeq \mathcal{E}(u)$ for $u \in \mathbb{R}^3$. It is convenient to identify $\Im(\mathbb{H}) = \mathbb{R}^3$, i. e. vectors are treated as purely imaginary quaternions and vice versa. The directors $d^1(p)$ and $d^2(p)$ span the rigid cross section of the rod. The third director $d^3(p)$ is always normal to the cross section, and its deviation from the direction

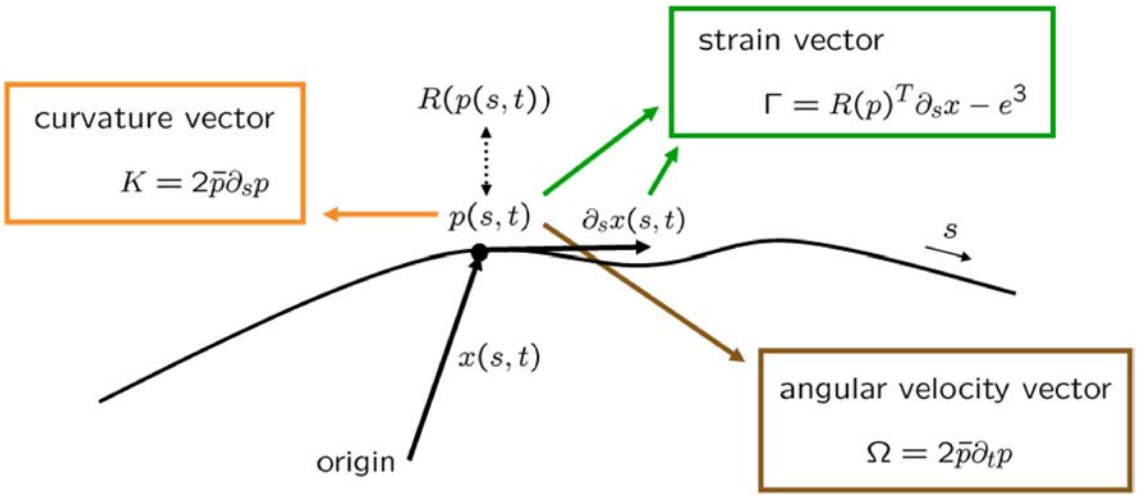

Figure 1: *The kinematical quantities of a continuous Cosserat rod.*

of the centerline tangent $\partial_s x$ indicates transverse shearing. As $R(\lambda p) = \lambda^2 R(p)$ holds for each $p \in \mathbb{H}$ and $\lambda \in \mathbb{R}$, the Euler map $p \mapsto R(p)$ given by (1) is sensitive w. r. t. stretching of p. In particular, (1) maps $\mathbb{S}^3$ into $SO(3)$, where $R(-p) = R(p)$ holds, such that p and its antipode $-p$ describe the same rotation. Conversely for each rotation Q in $SO(3)$ there exist exactly two unit quaternions — necessarily antipodes — that produce Q. So the unit sphere $\mathbb{S}^3$ covers $SO(3)$ exactly twice [23, 25, 34] via the Euler map. Stretched rotation can be expressed via quaternions as

$$R(p)v = pv\bar{p} \text{ (forward)} \quad \text{and} \quad R(p)^\top v = \bar{p}vp \text{ (backward)} \tag{2}$$

for $p \in \mathbb{H}$ and $v \in \Im(\mathbb{H}) = \mathbb{R}^3$, especially $d^i(p) = pe^i\bar{p} = R(p)e^i$ for each of the space fixed Euclidean base vectors e^1, e^2 and e^3 (classically denoted by 'i', 'j' and 'k') of $\Im(\mathbb{H}) = \mathbb{R}^3$. Recall that the quaternion product is defined by

$$pq = p_0 q_0 - \langle \hat{p}, \hat{q} \rangle + p_0 \hat{q} + q_0 \hat{p} + \hat{p} \times \hat{q} \qquad \text{for } p,\, q \in \mathbb{H}.$$

We use the symbols $p_0 = \Re(p)$ resp. $\hat{p} = \Im(p)$ to denote the real resp. the imaginary (= vector) part and $\bar{p} = p_0 - \hat{p}$ to denote the conjugate of a quaternion $p \in \mathbb{H}$. Note that $\bar{p} = \|p\|^2 p^{-1}$, where p^{-1} is the multiplicative inverse of p. Thus unit quaternions yield pure rotations without stretching. For details on the Hamilton quaternion division algebra, see [23].
In summary, the configuration of a Cosserat rod is determined by six degrees of freedom, all functions of the material coordinate s and time t: three translatory ones $x(s,t) \in \mathbb{R}^3$ locating the position of the cross section centroid on the centerline of the rod in space, and three rotatory ones $p(s,t) \in \mathbb{S}^3$ which fix the orientation of the material frame within the corresponding cross section of the rod. Correspondingly, there exist six objective strain measures which monitor the local change of these kinematical dof and determine the rod configuration up to an overall rigid body motion. From the viewpoint of the differential geometry, these are precisely the six differential invariants of a framed curve (see ch. III on moving frames in Cartan's book [15]).

Remark 2.1 (Kirchhoff rod models) In the structural mechanics of rods, also the classical model variants of Kirchhoff and Love [22, 36, 37, 42] have received considerable interest [16, 35, 44, 45, 48]. These variants may be obtained from the more general Cosserat model as described above by imposing additional *kinematical constraints* on the deformed rod configuration. An *'extensible Kirchhoff rod'* additionally satisfies the pair of constraints $\langle d^1, \partial_s x \rangle = \langle d^2, \partial_s x \rangle = 0$, which inhibits transverse shearing of the rod by confining the cross sections to remain normal to the centerline tangent. This reduces the number of dof from six to *four*. An *'inextensible Kirchhoff rod'* additionally satisfies $\|\partial_s x\| = 1$, which

implies that the centerline remains parametrised by arc length and inhibits longitudinal stretching (or compression) of the rod. Combining these constraints forces the centerline tangent to coincide with the cross section normal, i. e. $d^3 = \partial_s x$, which reduces the number of dof to *three*. □

2.1 Continuous potential energies and strain measures

The total potential energy $\mathcal{V} = \mathcal{V}_{SE} + \mathcal{V}_{BT}$ is additively decomposed into extensional and shearing energy $\mathcal{V}_{SE}$ and bending and torsion energy $\mathcal{V}_{BT}$. In $\mathcal{V}$, we include only the internal elastic energies, other conservative forces such as the gravitational force can simply be added as additional external forces on the right hand side of the balance equations. The **potential extensional** and **shearing energy** is given by

$$\mathcal{V}_{SE} = \frac{1}{2}\int_0^L \Gamma^\top C^\Gamma \Gamma \mathrm{d}s, \qquad C^\Gamma = \left(\begin{array}{c|ccc} 0 & & & \\ \hline & GA_1 & & \\ & & GA_2 & \\ & & & EA \end{array}\right), \tag{3}$$

where the *material strains* are defined by

$$\Gamma = R(p)^\top \partial_s x - e^3 = \bar{p}\partial_s x p - e^3. \tag{4}$$

Γ^1 resp. Γ^2 are the strains corresponding to shearing in d^1- resp. d^2-direction, Γ^3 is the strain corresponding to extension in d^3-direction. In components, we have

$$\Gamma^1 = \langle d^1(p), \partial_s x\rangle, \qquad \Gamma^2 = \langle d^2(p), \partial_s x\rangle, \qquad \Gamma^3 = \langle d^3(p), \partial_s x\rangle - 1. \tag{5}$$

$E > 0$ denotes Young's modulus and $G > 0$ the shear modulus of the material, $A = \iint_{\mathcal{A}} \mathrm{d}(\xi_1, \xi_2)$ is the area of the rigid cross section, $A_1 = \kappa_1 A$ and $A_2 = \kappa_2 A$ are some effective cross section areas with some Timoshenko shear correction factors $0 < \kappa_1, \kappa_2 \leq 1$, cf. [17]. Note that Γ is a vector (= purely imaginary quaternion) in $\mathbb{R}^3$, which we identify with $\Im(\mathbb{H})$. The **potential bending** and **torsion energy** is

$$\mathcal{V}_{BT} = \frac{1}{2}\int_0^L K^\top C^K K \,\mathrm{d}s, \qquad C^K = \left(\begin{array}{c|ccc} 0 & & & \\ \hline & EI_1 & & \\ & & EI_2 & \\ & & & GJ \end{array}\right), \tag{6}$$

where the *material curvature vector* is given by

$$K \simeq \mathcal{E}(K) = R(p)^\top \partial_s R(p). \tag{7}$$

K^1 resp. K^2 are the curvatures corresponding to bending around the d^1- resp. d^2-axis, K^3 is the curvature corresponding to torsion around the d^3-axis. Again, note that $K \in \mathbb{R}^3 = \Im(\mathbb{H})$.
The *'Darboux' vector* $k = RK = \sum_j K^j d^j$ is the spatial counterpart of the material curvature vector and appears in the generalised Frenet equations $\partial_s d^j = k \times d^j$, which describe the spatial evolution of the frame directors d^j along the centerline of the rod at fixed time.
The geometric moments of inertia of the rigid cross section $I_1 = \iint_{\mathcal{A}} \xi_2^2 \,\mathrm{d}(\xi_1, \xi_2)$ and $I_2 = \iint_{\mathcal{A}} \xi_1^2 \,\mathrm{d}(\xi_1, \xi_2)$ and the polar moment $J = I_3 = \iint_{\mathcal{A}} (\xi_1^2 + \xi_2^2) \,\mathrm{d}(\xi_1, \xi_2) = I_1 + I_2$ encode the geometrical properties of the cross section that enter into the stiffness constants of the potential energy (6). If the cross section is symmetric, then we have $I_1 = I_2$ and $J = I_3 = 2I_1 = 2I_2$. The *conservative elastic forces* F^Γ and *moments* M^K are derived from the potential energy as $F^\Gamma = C^\Gamma \Gamma = \frac{1}{2}\partial_\Gamma(\Gamma^\top C^\Gamma \Gamma)$ and $M^K = C^K K = \frac{1}{2}\partial_K(K^\top C^K K)$. Clearly, any other more general form of hyperelastic constitutive material behaviour could be used instead [26, 61]. If the rod possesses non-vanishing precurvature $K^0 : [0, L] \to \mathbb{R}^3$ in the undeformed configuration, K can simply be replaced by $K - K^0$ in (6) throughout the model [61].

Remark 2.2 (Hard and soft degrees of freedom) The slenderness of a typical rod geometry is characterised by the smallness of the parameter $\varepsilon = \sqrt{A}/L$ which measures the ratio of the linear dimension of the cross section to the length of a rod. As $I = \sqrt{I_1^2 + I_2^2} \simeq A^2$, an estimate of the relative order of magnitude of the potential energy terms (3) and (6) yields $\mathcal{V}_{BT}/\mathcal{V}_{SE} \simeq I/(AL^2) \simeq \varepsilon^2$. This explains the relative stiffness of a rod w. r. t. shearing and extension compared to bending and twisting deformations as a geometrical effect, independent of the material properties. □

It is well known that the strain measures (4) and (7) are objective (or *frame-indifferent*) quantities [38, 61]. It is likewise known [25, 39] that (7) is equivalent to

$$K = 2\bar{p}\partial_s p \tag{8}$$

provided that the quaternion p is of unit length. Identity (8) will turn out to be especially useful later, as we will use it to discretise the curvature directly on the level of quaternions. The geometry of $\mathbb{S}^3$ is used for interpolation purposes: Concerning rotations, cf. (1), it is completely 'isotropic' in the sense that no special direction is preferred. This property will make our discrete curvature measures frame-indifferent.

2.2 Continuous dissipation energies and strain rates

Our approach to model dissipation follows [2, 3]. We choose friction forces resp. moments that are proportional to the strain rates resp. curvature rates. The total dissipation energy $\mathcal{D} = \mathcal{D}_{SE} + \mathcal{D}_{BT}$ consists of dissipative extensional and shearing energy $\mathcal{D}_{SE}$ plus dissipative bending and torsion energy $\mathcal{D}_{BT}$. The **dissipative extensional** and **shearing energy** is

$$\mathcal{D}_{SE} = \int_0^L \dot{\Gamma}^\top C^{\dot{\Gamma}} \dot{\Gamma} \mathrm{d}s, \qquad C^{\dot{\Gamma}} = \left(\begin{array}{c|ccc} 0 & & & \\ \hline & c_1^{\dot{\Gamma}} & & \\ & & c_2^{\dot{\Gamma}} & \\ & & & c_3^{\dot{\Gamma}} \end{array}\right) \tag{9}$$

with the *material strain rates* $\dot{\Gamma} = \partial_t R(p)^\top \partial_s x + R(p)^\top \partial_{st}^2 x$. The **dissipative bending** and **torsion energy** is given by

$$\mathcal{D}_{BT} = \int_0^L \dot{K}^\top C^{\dot{K}} \dot{K} \,\mathrm{d}s, \qquad C^{\dot{K}} = \left(\begin{array}{c|ccc} 0 & & & \\ \hline & c_1^{\dot{K}} & & \\ & & c_2^{\dot{K}} & \\ & & & c_3^{\dot{K}} \end{array}\right) \tag{10}$$

with the *material curvature rates* $\dot{K} \simeq \partial_t \mathcal{E}(K) = \partial_t R(p)^\top \partial_s R(p) + R(p)^\top \partial_{st}^2 R(p)$. The nonnegative constants $c_i^{\dot{\Gamma}}$ and $c_i^{\dot{K}}$ for $i = 1, 2, 3$ denote some viscoelastic material parameters. The *dissipative damping forces* $F^{\dot{\Gamma}}$ and *moments* $M^{\dot{K}}$ are derived from the dissipation potential as $F^{\dot{\Gamma}} = 2C^{\dot{\Gamma}}\dot{\Gamma} = \partial_{\dot{\Gamma}}(\dot{\Gamma}^\top C^{\dot{\Gamma}} \dot{\Gamma})$ and $M^{\dot{K}} = 2C^{\dot{K}}\dot{K} = \partial_{\dot{K}}(\dot{K}^\top C^{\dot{K}} \dot{K})$. Of course, any other more general form of consistent viscoelastic constitutive material behaviour could replace these assumptions.

2.3 Continuous kinetic energies

The total kinetic energy $\mathcal{T} = \mathcal{T}_T + \mathcal{T}_R$ consists of two parts, the **translatory** $\mathcal{T}_T$ and the **rotatory** $\mathcal{T}_R$ **kinetic energy**, given by

$$T_T = \frac{\varrho A}{2} \int_0^L \|\dot{x}\|^2 \mathrm{d}s, \qquad T_R = \frac{\varrho}{2} \int_0^L \Omega^\top I \Omega \,\mathrm{d}s, \qquad I = \left(\begin{array}{c|ccc} 0 & & & \\ \hline & I_1 & & \\ & & I_2 & \\ & & & J \end{array}\right). \tag{11}$$

Here the *material angular velocity vector* (or the *'vorticity' vector*) is

$$\Omega \simeq \mathcal{E}(\Omega) = R(p)^\top \partial_t R(p). \tag{12}$$

In (11), $\varrho > 0$ is the mass density per volume, I_1, I_2 and $J = I_3$ are as above, and we identify $\Omega \simeq \mathcal{E}(\Omega)$. Note again that $\Omega \in \mathbb{R}^3 = \Im(\mathbb{H})$. The kinetic energy takes on the special form (11), since it is assumed that the rod centerline x passes through the centers of mass and the directors d^1, d^2 are aligned in parallel to the geometric principal directions of inertia of the cross sections [61].

We rewrite the rotatory kinetic energy with the identity $\Omega^\top I\Omega = \dot p^\top \mu(p)\dot p$ and the p dependent 4×4 quaternion mass matrix

$$\mu(p) = 4\mathcal{Q}(p)I\mathcal{Q}(p)^\top, \qquad \mathcal{Q}(p) = \left(\begin{array}{c|c} p_0 & -\hat p^\top \\ \hline \hat p & p_0\mathcal{I} + \mathcal{E}(\hat p)\end{array}\right) = \left(\begin{array}{c|ccc} p_0 & -p_1 & -p_2 & -p_3 \\ \hline p_1 & p_0 & -p_3 & p_2 \\ p_2 & p_3 & p_0 & -p_1 \\ p_3 & -p_2 & p_1 & p_0\end{array}\right) \tag{13}$$

Details are carried out in [9, 39, 56] and the references cited therein. In that context, $\mathcal{Q}(p)$ is sometimes called the 'quaternion matrix' corresponding to $p\in\mathbb{H}$, since it allows to express the product of p with another quaternion $q\in\mathbb{H}$ as a matrix-vector product, i. e. $pq = \mathcal{Q}(p)q$. The mass matrix satisfies the symmetry property $\mu(-p) = \mu(p)$, which is a consequence of the fact that both p and $-p$ describe the same rotation $R(p) = R(-p)$. The kernel of $\mu(p)$ is given by $\ker\mu(p) = \mathbb{R}p$, consequently we have $\operatorname{rk}\mu(p)$ equal to three. The matrix $\mu(p)$ is positively semi-definite with the one singular dimension in direction p.

Similarly as for the curvature, equation (12) for the angular velocity can be rewritten directly in terms of the unit quaternion p, namely,

$$\Omega = 2\bar p\partial_t p, \tag{14}$$

see [38, 63]. The reader should note that the situation for K and Ω is completely analogous from a two dimensional field view. For our discrete model, evolution (8) is the basis for spatial discretisation. Evolution (14) is solved 'continuously' in time, of course.

2.4 Continuous equations of motion

It can be shown [39] that the unknowns $x(s,t)$ and $p(s,t)$ of a Cosserat rod, for given exterior material force densities $\hat F = \hat F(t)$ (per length) and given exterior material moment densities $\hat M = \hat M(t)$ (per length), satisfy the following nonlinear system of partial differential-algebraic equations,

$$\left\{\begin{array}{rcl} \varrho A\ddot x &=& \partial_s(pF\bar p) + p\hat F\bar p \\ \varrho\Big[\mu\ddot p - \frac{1}{2}\partial_p\big(\dot p^\top\mu\dot p\big) + \partial_p\big(\mu\dot p\big)\dot p\Big] &=& 2\big(x'pF + \partial_s(pM) + p'M + p\hat M\big) - \lambda p \\ 0 &=& \|p\|^2 - 1 \end{array}\right. . \tag{15}$$

The first equation (15_1) corresponds to the balance of linear momentum, the second one (15_2) to the balance of angular momentum. Here $' = \partial_s$, $\dot{} = \partial_t$, $\mu = \mu(p)$ from (13) and $\lambda : [0,L]\times[0,T]\to\mathbb{R}$, $(s,t)\mapsto\lambda(s,t)$ denote some Lagrange multipliers, which must be introduced as additional unknowns because of the presence of the normality condition for the quaternions [39]. Together with appropriate initial and boundary conditions, this is the system that has to be solved for the unknowns x, p and λ. In (15), the viscoelastic forces and moments are given by $F = C^\Gamma\Gamma + 2C^{\dot\Gamma}\dot\Gamma$ and $M = C^K K + 2C^{\dot K}\dot K$ due to the constitutive assumptions. Hence, in the undamped — purely elastic and conservative — case, the shearing forces F^1, F^2, the extensional force F^3, the bending moments M^1, M^2 and the torsional moment M^3 are related to the shearing strains Γ^1, Γ^2, the extensional strain Γ^3, the bending curvatures K^1, K^2 and the torsional curvature K^3 via

$$F^1 = GA_1\Gamma^1, \quad F^2 = GA_2\Gamma^2, \quad F^3 = EA\Gamma^3, \quad M^1 = EI_1K^1, \quad M^2 = EI_2K^2, \quad M^3 = GJK^3. \tag{16}$$

Originally in [61, 62], averaging the normal Piola-Kirchhoff tractions and corresponding torques over the cross section of the deformed rod, it was shown that the Cosserat rod must satisfy the following spatial form of the balance equations of motion, namely

$$\left\{\begin{array}{rcl} \varrho A\,\ddot x &=& \partial_s f + \hat f \\ \varrho\big(i\dot\omega + \omega\times i\omega\big) &=& \partial_s m + \partial_s x\times f + \hat m \end{array}\right. . \tag{17}$$

This original formulation of the equations of motion, which is probably more familiar to the reader, can as well be found in [2, 3]. Here the spatial quantities

$$\gamma = R\Gamma, \quad k = RK, \quad \omega = R\Omega, \quad i = RIR^\top, \quad f = RF, \quad m = RM, \quad \hat f = R\hat F, \quad \hat m = R\hat M \tag{18}$$

are obtained from the corresponding material ones by a '*push forward*' rotation via R. The components of any of these spatial quantities in the moving coordinate system (d^1, d^2, d^3) are identical to the components of the corresponding material quantities, measured in the fixed global coordinate system (e^1, e^2, e^3).

It can be shown that the systems (15) and (17) are equivalent. As the reader might feel unfamiliar with (15), we briefly sketch the simplest way, how (15) can be derived from the common system (17). The simplest way to show this is to insert (18) into (17) in order to obtain the material form

$$\left\{\begin{array}{rcl} \varrho A\,\ddot{x} &=& \partial_s(RF) + R\hat{F} \\ \varrho R\big(I\dot{\Omega} + \Omega \times I\Omega\big) &=& \partial_s(RM) + \partial_s x \times (RF) + R\hat{M} \end{array}\right. \tag{19}$$

from the spatial form (17) of the balance equations, to let $R = R(p)$ with the Euler map (1) and to use the basic properties (2), the angular velocity expression (14), the hidden constraints $\langle p, \dot{p}\rangle = 0$ and $\langle p, \ddot{p}\rangle = -\|\dot{p}\|^2$ and straightforward quaternion algebra. The details are not difficult, but rather lengthy. They are carried out step-by-step in [39]. Alternatively, the quaternionic formulation (15) of the balance equations (17) can be derived from a two-dimensional variational principle in the variable (s, t). This is not topic of the present paper, but the interested reader is referred to [39] for a detailed exposition.

Before finishing this section, let us briefly explain, how (15) can be solved for the quaternionic acceleration $\ddot{p}$. To that end, let $\mu(p)^\sharp$ for $p \in \mathbb{H}$ denote the matrix

$$\mu(p)^\sharp = 4\mathcal{Q}(p) I^\sharp \mathcal{Q}(p)^\top, \qquad I^\sharp = \left(\begin{array}{c|ccc} 0 & & & \\ \hline & I_1^{-1} & & \\ & & I_2^{-1} & \\ & & & J^{-1} \end{array}\right).$$

The matrix $\mu(p)^\sharp$ is 'almost' an inverse of the radially singular mass $\mu(p)$: Actually, it satisfies the property $\mu(p)^\sharp \mu(p) = \mathcal{I} - p \otimes p$, this is $\mu(p)^\sharp \mu(p)\pi = \pi - \langle p, \pi\rangle p$ for each $p \in \mathbb{S}^3$ and $\pi \in \mathbb{H}$. This means that $\mu^\sharp \mu$ extracts the tangential part of π. Now, if we left-multiply (15_2) with $\mu(p)^\sharp$, the d'Alembert constraint forces λp at the right-hand side are eliminated, since $\ker \mu(p)^\sharp = \mathbb{R}p$. If we use the constraint $\langle p, \ddot{p}\rangle = -\|\dot{p}\|^2$ for the quaternionic normal acceleration, we end up in the system

$$\left\{\begin{array}{rcl} \ddot{x} &=& \dfrac{1}{\varrho A}\Big(\partial_s(pF\bar{p}) + p\hat{F}\bar{p}\Big) \\ \ddot{p} &=& \dfrac{2}{\varrho}\mu(p)^\sharp\Big(4\varrho\dot{p}I\dot{\bar{p}}p + x'pF + \partial_s(pM) + p'M + p\hat{M}\Big) - \|\dot{p}\|^2 p \end{array}\right. . \tag{20}$$

Here as well the helpful identity $\frac{1}{2}\partial_p(\dot{p}^\top \mu(p)\dot{p}) - \partial_p(\mu(p)\dot{p})\dot{p} = 8\varrho\dot{p}I\dot{\bar{p}}p$, see [39, 56], was used. In fact, system (20) is equivalent to (15). Hence, it is also equivalent to (17). In section 3.4, we will demonstrate that the finite difference discretisation schemes, which we propose, are consistent to (20).

3 Discrete Cosserat rods via finite differences and quotients

Here we present our discrete version of the Cosserat model. Sections 3.1, ..., 3.4 are the discrete counterparts of sections 2.1, ..., 2.4 respectively.
Contrasting the more frequently applied finite element approach (see e.g. [64]), we propose the following staggered grid discretisation. We subdivide the arc length interval $[0, L]$ into N segments $[s_{n-1}, s_n]$ with the vertices $0 = s_0 < s_1 < \ldots < s_{N-1} < s_N = L$. Together with the segment midpoints $s_{n-1/2} = (s_{n-1} + s_n)/2$ we obtain the staggered grid $0 = s_0 < s_{1/2} < s_1 < \ldots < s_{N-1} < s_{N-1/2} < s_N = L$, on which the various kinematical quantities of our discrete Cosserat rod model reside.
We associate the discrete **translatory degrees of freedom** $x_n : [0, T] \to \mathbb{R}^3$, i. e. the cross section centroids, to the vertices, $x_0(\cdot) \approx x(s_0, \cdot)$, ..., $x_N(\cdot) \approx x(s_N, \cdot)$, and the discrete **rotatory degrees of freedom** $p_{n-1/2} : [0, T] \to \mathbb{H}$, i. e. the quaternions specifying the frame orientations, on the segment midpoints, $p_{1/2}(\cdot) \approx p(s_{1/2}, \cdot)$, ..., $p_{N-1/2}(\cdot) \approx p(s_{N-1/2}, \cdot)$, so the corresponding frames $R(p_{n-1/2})$ and

directors $d^i(p_{n-1/2})$ likewise live on the midpoints. In order that the quaternions remain in $\mathbb{S}^3$, we have to introduce the discrete **Lagrange multipliers** $\lambda_{n-1/2} : [0,T] \to \mathbb{R}$, situated on the midpoints, $\lambda_{1/2}(\cdot) \approx \lambda(s_{1/2}, \cdot)$, ... $\lambda_{N-1/2}(\cdot) \approx \lambda(s_{N-1/2}, \cdot)$ and N constraints $0 = g_{n-1/2}(q)$ with $2g_{n-1/2}(q) = \|p_{n-1/2}\|^2 - 1$, which are situated here as well.

A staggered grid discretisation using quaternionic dof was already proposed in [21] for the case of an inextensible Kirchhoff rod formulated as a Hamiltonian system. We extend this idea to shearable and extensible Cosserat rods in the Lagrangian setting. Due to the relative stiffness of the extensional and shearing dof (cf. remark 2.2), the staggered grid approach permits an interpretation of the rod as a sequence of almost rigid cylinders, connected with appropriate 'bushings' for bending and torsion. We consequently use the notation $\cdot_n$ for quantities at the vertices s_n; here n ranges from 0 to N. We use the notation $\cdot_{n-1/2}$ for quantities that are situated on the midpoints $s_{n-1/2}$; here n ranges from 1 to N, if not otherwise explicitly stated. The situation is depicted in Figure 2.

In the sequel, we discretise the continuous internal Cosserat energy integrals $\mathcal{V}$, $\mathcal{T}$ and $\mathcal{D}$ by the use of either midpoint or trapezoidal quadrature, depending on where which quantity ist 'at home'. The weight factors for the midpoint rule are the segment lengths $\Delta s_{n-1/2} = s_n - s_{n-1}$. Likewise, the weights for the trapezoidal rule are the lengths of the bucked segments $2\delta s_0 = \Delta s_{1/2}$, $2\delta s_n = \Delta s_{n-1/2} + \Delta s_{n+1/2}$ and $2\delta s_N = \Delta s_{N-1/2}$. Then, with the discrete degrees of freedom $q = (x_0, p_{1/2}, x_1, \ldots, x_{N-1}, p_{n-1/2}, x_N)$, the discrete potential energy $\mathcal{V}$, the discrete kinetic energy $\mathcal{T}$, the discrete dissipation energy $\mathcal{D}$, the discrete constraints $g = (g_{1/2}, \ldots, g_{n-1/2})$, the discrete Lagrange multipliers $\lambda = (\lambda_{1/2}, \ldots, \lambda_{N-1/2})$, the discrete Lagrange function $\mathcal{L} = \mathcal{T} - \mathcal{V} - g^\top \lambda$ and given discrete exterior forces $\hat{\mathcal{F}}(t)$, the variational principle

$$\delta \int_0^T \mathcal{L}\,\mathrm{d}t - \int_0^T \partial_{\dot q}\mathcal{D}\,\delta q\,\mathrm{d}t + \int_0^T \hat{\mathcal{F}}\,\delta q\,\mathrm{d}t = 0$$

yields the Euler-Lagrange equations as the well-known *index three* differential algebraic system of equations

$$\left\{ \begin{array}{rcl} \mathcal{M}(q)\ddot q &=& \mathcal{F}(q,\dot q,t) - \mathcal{G}(q)^\top \lambda \\ 0 &=& g(q) \end{array} \right. \tag{21}$$

with the right hand side forces given by $\mathcal{F}(q,\dot q,t) = \hat{\mathcal{F}}(t) - \partial_q \mathcal{V}(q,t) - \partial_{\dot q}\mathcal{D}(q,\dot q,t) + \frac{1}{2}\partial_q(\dot q^\top \mathcal{M}(q)\dot q) - \partial_q(\mathcal{M}(q)\dot q)\dot q$, cf. [4, 29].

Throughout the remainder of this section, we address the discrete counterparts of the corresponding continuous quantities of the preceding section, and consistently drop the adjective 'discrete' from now on. For both a continuous quantity and its (spatially) discrete version, we use the same symbol: So for example, the continuous Lagrange multiplier λ of the preceding section is a function defined on the rectangular domain $[0,L]\times[0,T]$, whereas its discretisation is represented by the vector $\lambda = (\lambda_{1/2}, \ldots, \lambda_{N-1/2})$, with each component $\lambda_\cdot$ being a function defined on the interval $[0,T]$.

Next we discuss the adequate formulation of the dynamical equations in view of the methods we intend to apply for their numerical integration. One method is to use eight local charts $p_k = \pm(1 - \sum_{j\neq k} p_j^2)^{1/2}$ for $k = 0, \ldots, 3$ that cover the unit sphere $\mathbb{S}^3 = \partial B_1^{\mathbb{H}}(0) \subset \mathbb{H}$. Numerical approaches using local charts exist [29], however, changing charts is a tedious task and it is much easier to formulate the equations of motion as a system of differential algebraic equations, where we keep the quaternion unity condition $2g = \|p\|^2 - 1 = 0$ as a hard algebraic constraint. It is well known that the numerical solution of the index three system involves difficulties such as poor convergence of Newton's method [4, 24, 27, 29, 60], so we reduce the index to one

$$\begin{pmatrix} \ddot q \\ \lambda \end{pmatrix} = \begin{pmatrix} \mathcal{M}(q) & \mathcal{G}(q)^\top \\ \mathcal{G}(q) & 0 \end{pmatrix}^{-1} \begin{pmatrix} \mathcal{F}(q,\dot q,t) \\ -\partial^2_{qq} g[\dot q,\dot q] \end{pmatrix} \tag{22}$$

and solve the index zero subsystem $\ddot q = \ddot q(q,\dot q,t)$. Stabilisation of the quaternion unity constraints in the index one/zero case is especially easy and cheap.

Remark 3.1 (Boundary conditions) In order to apply clamped boundary rotations properly, i. e. $p_0 = p_0(t)$ and $p_N = p_N(t)$, we introduce virtual *ghost* quaternions $p_{-1/2}$ and $p_{N+1/2}$, which is a standard technique [47]. They are situated beyond the boundary and defined as the spherical linear extrapolation of

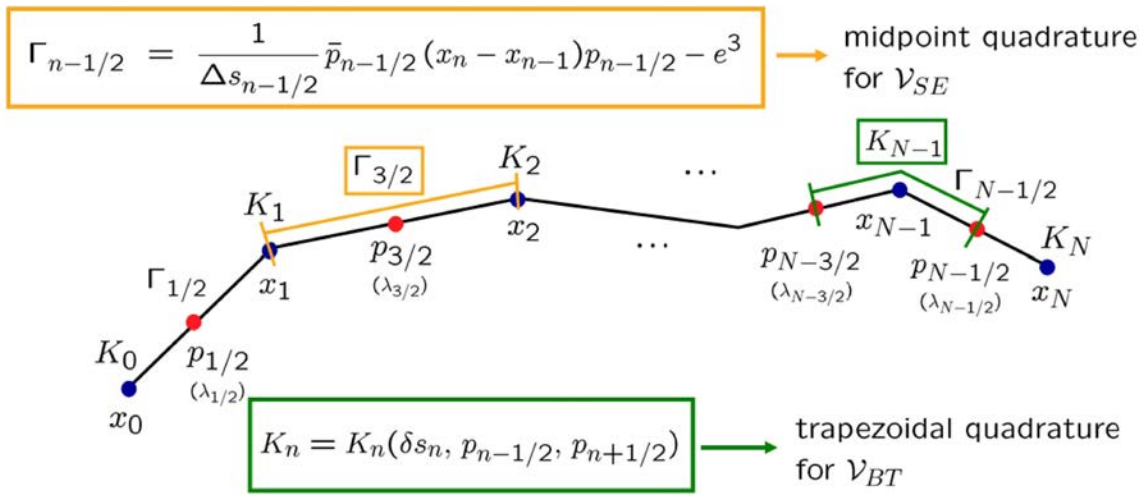

Figure 2: *The 'staggered grid' finite difference discretisation of a Cosserat rod.*

$p_{1/2}$ via $p_0(t)$ or $p_{N-1/2}$ via $p_N(t)$ respectively. The handling of free boundary conditions with vanishing boundary curvature and moment is clear. □

3.1 Discrete potential energies and strain measures

We start with the discrete version of the **potential extensional** and **shearing energy**. As the strains $\Gamma_{n-1/2}$ are located on the midpoints, we approximate the integral (3) using the midpoint rule,

$$\mathcal{V}_{SE} = \frac{1}{2}\sum_{n=1}^{N} \Delta s_{n-1/2} \Gamma_{n-1/2}^{\top} C^{\Gamma} \Gamma_{n-1/2}, \qquad \Gamma_{n-1/2} = R(p_{n-1/2})^{\top} \frac{\Delta x_{n-1/2}}{\Delta s_{n-1/2}} - e^3, \tag{23}$$

where $\Gamma_{n-1/2}$ denote the *discrete material strains*. They locally depend on $\Delta x_{n-1/2} = x_n - x_{n-1}$ and $p_{n-1/2}$, see Figure 2.
We continue with the discrete version of the **potential bending** and **torsion energy**. The curvatures K_n are located on the vertices, so we approximate (6) with the trapezoidal rule

$$\mathcal{V}_{BT} = \frac{1}{2}\sum_{n=0}^{N} \delta s_n K_n^{\top} C^{K} K_n, \qquad K_n = K_n(\delta s_n,\, p_{n-1/2}, p_{n+1/2}), \tag{24}$$

where the *discrete material curvatures* K_n depend on $R(p_{n-1/2})$ and $R(p_{n+1/2})$, see Figure 2. The choice K_n of an appropriate curvature measure is by no means unique. To simplify matters, we restrict ourselves to the equidistant case in the following. Frame indifference requires that the discrete curvature K_n is function of the 'finite quotient' $R(p_{n-1/2})^{\top} R(p_{n+1/2})$ or — equivalently — $\bar{p}_{n-1/2} p_{n+1/2}$ [12, 33]. Next we have to consider the problem how to interpolate the two quaternions $p_{n-1/2}$ resp. $p_{n+1/2}$ located at the segment midpoints $s_{n-1/2}$ resp. $s_{n+1/2}$ to obtain a quaternion p_n defined at the vertex at s_n, and how to choose an appropriate finite difference expression $\delta p_n / \delta s_n$ in order to approximate the quaternionic curvature expression $K = 2\bar{p}\,\partial p/\partial s$, see (8), at the vertex s_n by an expression of the type

$$K(s_n) \;=\; 2\bar{p}\frac{\partial p}{\partial s}\bigg|_{s=s_n} \;\approx\; 2\bar{p}_n \frac{\delta p_n}{\delta s_n} \;=\; K_n \quad . \tag{25}$$

Below we present five possible choices, which are inspired by expressions appearing in an identical or a similar form elsewhere in the literature [6, 12, 20, 53, 59, 63]. All of them have in common that they lead

to the following 'finite quotient' expression

$$K_n = \frac{2}{\delta s_n}\zeta(\theta_n)\Im(W_n), \qquad \theta_n = \arccos\Re(W_n), \qquad W_n = \bar{p}_{n-1/2}p_{n+1/2} \tag{26}$$

with different scalar characteristic weighting functions $\zeta = \zeta(\theta)$,

$$\text{(i)}\ \ \zeta(\theta) = 1, \qquad \text{(ii)}\ \ \zeta(\theta) = \sqrt{\frac{2}{1+\cos\theta}}, \qquad \text{(iii)}\ \ \zeta(\theta) = \frac{1}{\cos\theta},$$

$$\text{(iv)}\ \ \zeta(\theta) = \frac{2}{1+\cos\theta}, \qquad \text{(v)}\ \ \zeta(\theta) = \frac{\theta}{\sin\theta}$$

In (26), W_n is the quotient quaternion, i.e. $p_{n+1/2}$ left-divided by $p_{n-1/2}$, and θ_n is the angle between $p_{n-1/2}$ and $p_{n+1/2}$ in the quaternionic space $\mathbb{H}$. Note that $\theta_n = \arccos\langle p_{n-1/2}, p_{n+1/2}\rangle$. It is easy to see that W_n is frame indifferent; this can be done exactly in the same way as in the continuous case [38]. Consequently, $\Re(W_n)$, $\Im(W_n)$ and thus θ_n and K_n are frame indifferent. In fact, 'finite quotients' are the natural 'finite differences' on the quaternionic unit sphere $\mathbb{S}^3 \subset \mathbb{H}$, since that subgroup is of *multiplicative* nature (non-commutative rotations!).
As $2\Im(W_n) = W_n - \bar{W}_n = \bar{p}_{n-1/2}p_{n+1/2} - \bar{p}_{n+1/2}p_{n-1/2}$ and $\cos(\theta_n) = \Re(W_n) = (W_n + \bar{W}_n)/2$, one likewise recognises that all of the above variants of the weighting function $\zeta(\theta)$ lead to simple algebraic expressions of the discrete curvature K_n as given by (26) in terms of the adjacent midpoint quaternions $p_{n\pm1/2}$.
It can be shown that each of the above variants (i) to (v) of (26) may be obtained by inserting a specific choice of the interpolated vertex quaternion p_n combined with a suitable FD expression δp_n in terms of the midpoint quaternions $p_{n\pm1/2}$ into the FD approximation (25), such that (26) constitutes a consistent FD approximation of the curvature at the vertices. For details, see the appendix. The proposed curvatures can be interpreted in terms of so-called 'vectorial parametrisations' [6] of the quotient W_n. In the terminology of [6], curvatures (i), (iii), (iv) resp. (v) are related to the 'reduced Euler-Rodrigues', 'Cayley-Gibbs-Rodrigues', 'Wiener-Milenkovic' resp. 'rotation vector' parametrisations of W_n.

3.2 Discrete dissipation energies and strain rates

The discretisation of the dissipation potential has to be consistent with the discretisation of the potential energies. We start with the **dissipative extensional** and **shearing energy**. The strain rates $\dot{\Gamma}_{n-1/2}$ are located at the midpoints. Thus, the continuous integral (9) is approximated with the midpoint rule,

$$\mathcal{D}_{SE} = \sum_{n=1}^{N} \Delta s_{n-1/2}\dot{\Gamma}_{n-1/2}^{\top} C^{\dot{\Gamma}}\, \dot{\Gamma}_{n-1/2}, \qquad \dot{\Gamma}_{n-1/2} = \frac{\partial}{\partial t}\Gamma_{n-1/2},$$

where the *discrete material strain rates* are given by the time derivative of (23). They depend both on the positions x_{n-1}, x_n, $p_{n-1/2}$ and the velocities $\dot{x}_{n-1}$, $\dot{x}_n$, $\dot{p}_{n-1/2}$. Concerning the discrete **dissipative bending** and **torsion energy**, the curvature rates $\dot{K}_n$ are situated — like the curvatures themselves — on the vertices. Thus, (10) is approximated with a trapezoidal sum,

$$\mathcal{D}_{BT} = \sum_{n=0}^{N} \delta s_n \dot{K}_n^{\top} C^{\dot{K}} \dot{K}_n, \qquad \dot{K}_n = \frac{\partial}{\partial t}K_n,$$

where the *discrete material curvature rates* are the time derivative of (24), depending on $p_{n-1/2}$, $p_{n+1/2}$ and $\dot{p}_{n-1/2}$, $\dot{p}_{n+1/2}$.

3.3 Discrete kinetic energies

As the centroids x_n are situated at the vertices s_n, we discretise the **translatory kinetic energy** integral in (11) by the trapezoidal rule and, as the quaternions $p_{n-1/2}$ are situated on the midpoints $s_{n-1/2}$, the

rotatory kinetic energy integral (11) is approximated with the midpoint rule,

$$\mathcal{T}_T = \frac{\varrho A}{2}\sum_{n=0}^{N}\delta s_n\|\dot{x}_n\|^2, \qquad \mathcal{T}_R = \frac{\varrho}{2}\sum_{n=1}^{N}\Delta s_{n-1/2}\dot{p}_{n-1/2}^{\top}\mu(p_{n-1/2})\dot{p}_{n-1/2}. \tag{27}$$

Thus, the translatory mass is concentrated at the vertices, and the corresponding rotatory inertia terms belong to the quaternions located at the segment midpoints. The *discrete material angular velocities* $\Omega_{n-1/2} = 2\bar{p}_{n-1/2}\dot{p}_{n-1/2}$ as well belong to the midpoints. Since the masses are lumped, the mass matrix $\mathcal{M}(q)$ of the system becomes block diagonal with alternating 3×3 (translatory, diagonal and constant) and 4×4 (rotatory, position-dependent) blocks.
Each summand in (27) can be interpreted as the rotatory energy of a rigid body with moments of inertia equal to $\bar{I}^1 = \varrho\Delta s I_1$, $\bar{I}^2 = \varrho\Delta s I_2$ and $\bar{I}^3 = \varrho\Delta s I_3$, see [50, 56]. These are in fact the physical moments of inertia of a disc with vanishing thickness. Now we consider the rod as decomposed into N — almost rigid — cylinders with moments of inertia, which we denote by I^1, I^2 and I^3. Comparison shows that $I^i - \bar{I}^i = \mathcal{O}(\Delta s^3)$ for $i = 1, 2$, and $I^3 - \bar{I}^3 = 0$. For fine discretisations, these defects may be neglected. Otherwise, a more detailed modelling of the rotatory inertia terms may be required.
For each centroid x_n with mass $\varrho A\delta s_n$, the translatory mass-matrix block is given by a 3×3 diagonal, constant, state independent block $\varrho A\delta s_n\mathcal{I}$. For the rotatory part, we fix a segment $\Delta s = \Delta s_{n-1/2}$ and its quaternion $p = p_{n-1/2}$. The constraints of position, velocity and acceleration are written $2g = \|p\|^2 - 1 = 0$, $\dot{g} = G(p)\dot{p} = \langle p, \dot{p}\rangle = 0$ and $\ddot{g} = G(p)\ddot{p} + \partial^2_{pp}g[\dot{p},\dot{p}] = \langle p, \ddot{p}\rangle + \|\dot{p}\|^2 = 0$ respectively, where $G(p) = \partial_p g(p) = p^{\top}$. Thus, the rotatory quaternion mass-constraint-matrix 5×5 block is given by

$$\left(\begin{array}{c|c} \varrho\Delta s\mu(p) & G(p)^{\top} \\ \hline G(p) & 0 \end{array}\right) = \left(\begin{array}{c|c} \varrho\Delta s\mu(p) & p \\ \hline p^{\top} & 0 \end{array}\right) \tag{28}$$

with the singular quaternion mass $\mu(p)$ from (13). The inverse of (28) exists iff $p \neq 0$ and can be explicitly algebraically computed. It has exactly the same structure as (28), where $\varrho\Delta s\mu(p)$ is simply replaced by $\frac{1}{\varrho\Delta s}\mu(p)^{\sharp}$, and it can therefore be calculated at exactly the same numerical cost [38, 39].
The question arises, why to use $p_{n-1/2}$ and $\dot{p}_{n-1/2}$ as the primary unknowns and not $p_{n-1/2}$ and $\Omega_{n-1/2}$, as recommended by some authors [56, 63]. The reason is that many standard ODE or DAE solvers such as RADAU5, SEULEX or RODAS [27, 29, 43] support sparse / banded linear algebra that is specially adapted to second order systems of the form $\dot{q} = v$, $\dot{v} = \dot{v}(q, v, t)$. An elaborate discussion on that question can be found in [38].

Remark 3.2 (Condition) It can be shown that the condition number of the mass-constraint matrix (28) is equal to the ratio $\max M/\min M$, where $M = \{\varrho\Delta s I_1, \varrho\Delta s I_2, \varrho\Delta s I_3, 1/4\}$. So, for typical material parameters and discretisations, the system is rather ill-conditioned. By scaling the constraint equation by a factor of $c > 0$, the condition number of any quaternion mass-constraint block (28) can be influenced. If g is replaced by cg, G has to be replaced by cG and $\partial^2_{pp}g$ by $c\partial^2_{pp}g$. For the special case of symmetric cross sections for example, where $I_1 = I_2 = I$, $J = I_1 + I_2 = 2I$, any choice $c \in 4\varrho\Delta s[I, J]$ leads to a condition number of two. Note that the Lagrange multiplier λ scales with $1/c$, so that the constraint force $G^{\top}\lambda$, which — in accordance to d'Alembert's principle — is normal to the unit sphere and keeps the quaternions on its spherical orbit, remains unchanged. For more sophisticated rescaling techniques, the reader is referred to [5]. □

Remark 3.3 (Constraint stabilisation) For the index zero/one formulation (22), the position q drifts quadratically from the constraint manifold $\{q : g(q) = 0\}$. Subsequent *projection* $p \mapsto p/\|p\|$ of the quaternion position and $\dot{p} \mapsto \dot{p} - \langle p, \dot{p}\rangle p$ of the quaternion velocity is especially cheap, it may be applied even after each successful integration step. However, easy and efficient implementations of this method are restricted to one step integration methods, excluding BDF methods with order of at least two.
Another stabilisation technique applied already on the model level is the *Baumgarte method* [29]. Imposing the linear combinations $\ddot{g} + 2r\dot{g} + \omega^2 g = 0$ as constraints with $\omega, r > 0$, the index one Baumgarte formulation is obtained. The equation for the Lagrange multiplier λ remains unchanged. The additional penalty accelerations are needed to pull p back to $\mathbb{S}^3$, if the velocity constraint $\langle p, \dot{p}\rangle = 0$ or the position

constraint $\|p\|^2 = 1$ is violated. The choice $r = \omega$ leads to critical damping of the constraint defect g. It is known that the Baumgarte method introduces an artificial dissipation of energy, but this is the case for projection methods as well [29, 30]. Another objection to the Baumgarte method concerns the introduction of additional stiffness into the system. As in our case the Cosserat shearing and extensional 'springs' are already stiff, this does not constitute a drawback from the practical viewpoint [38]. □

3.4 Discrete equations of motion

Carrying out the details of the preceding sections and plugging all the pieces together, we obtain the discrete translatory and rotatory balance equations in ODE form. Using the index notation $n = 0, \ldots, N$ and $\nu = 1/2, \ldots, N-1/2$ and, to simplify matters, considering the equidistant case, we obtain the system

$$\left\{\begin{array}{lcl} \ddot{x}_n &=& \dfrac{1}{\varrho A \delta s_n}\Big(p_{n+\frac{1}{2}} F_{n+\frac{1}{2}} \bar{p}_{n+\frac{1}{2}} - p_{n-\frac{1}{2}} F_{n-\frac{1}{2}} \bar{p}_{n-\frac{1}{2}}\Big) \\ \ddot{p}_\nu &=& \dfrac{2}{\varrho \Delta s_\nu} \mu(p_\nu)^\sharp \Big(4\varrho \Delta s_\nu \dot{p}_\nu I \dot{\bar{p}}_\nu p_\nu + \Delta x_\nu p_\nu F_\nu + p_{\nu+1} M_{\nu+\frac{1}{2}} - p_{\nu-1} M_{\nu-\frac{1}{2}}\Big) - \|\dot{p}_\nu\|^2 p_\nu \end{array}\right. \tag{29}$$

with the internal forces $F_\cdot = C^\Gamma \Gamma_\cdot + 2C^{\dot\Gamma}\dot\Gamma_\cdot$ and moments $M_\cdot = C^K K_\cdot + 2C^{\dot K}\dot K_\cdot$. The system (29) is of the form

$$\dot u = f(u,t), \qquad u = (q,v), \qquad q = (x_0, p_{1/2}, x_1, \ldots, x_{N-1}, p_{N-1/2}, x_N), \qquad v = \dot q \tag{30}$$

and constitutes the index zero subsystem, which is obtained by discarding the equations for the Lagrange multipliers in (22). It can be solved by any ODE integrator, with an appropriate technique to avoid the drift-off effect. If the Lagrange multipliers are of interest, they can be obtained from (29) as $\lambda_\nu = \big\langle 2p_\nu, 4\varrho\Delta s_\nu \dot p_\nu I \dot{\bar p}_\nu p_\nu + \Delta x_\nu p_\nu F_\nu + p_{\nu+1} M_{\nu+\frac{1}{2}} - p_{\nu-1} M_{\nu-\frac{1}{2}}\big\rangle$.
Comparing (29) to its continuum counterpart (20) it can be seen that (29) yields a consistent discretisation of (20) in the equidistant case.
We wish to note that, starting from a variational formulation of the model also in the discrete case, our discrete balance equations (29) contain a favourable discretisation of the continuum terms $\partial_s(pF\bar p)$ and $\partial_s(pM)$ in conservation form on the staggered grid.
Yet, proofs of stability and convergence are still an open topic that deserve to be studied analytically. Numerical experiments [38] confirm that (29) yields a second order accurate discretisation of the continuous equations (20).
Note that in (29), exterior material forces $\hat F(t)$ — the gravitational force for example — and material moments $\hat M(t)$ can be easily added on the right hand side of these equations. The topological structure of the system results in upper and lower bandwidths of the quadratic Jacobians $\partial\dot v/\partial q$ and $\partial\dot v/\partial\dot q$ equal to ten [38].
The reader should observe that, intrinsically in the model, there are many common terms and — quaternionic skew — symmetries. This is one reason, why the model can be implemented with very few arithmetic operations. So, the basic model with curvature (i) needs about $581N$ basic arithmetic operations — i. e. just additions, subtractions, multiplications and divisions —, where N is the number of segments, see Table 1. All in all, the evaluation cost for f and $\partial f/\partial u$ is thus extremely small.

Remark 3.4 (Kirchhoff rod models) In certain applications one is interested solely in the proper modeling of bending and torsion. Also, stiff extensional and shearing springs deteriorate the computational performance considerably. If possible, such stiff components should be avoided by model reduction [60]. In our case, extensible as well as inextensible Kirchhoff rods can be incorporated easily by introducing additional constraints $g^i_{n-1/2} = \Gamma^i_{n-1/2}$, $i = 1, 2(, 3)$. For the boundary conditions, the handling of t-dependent constraints is explained in [4, 38]. The advantage is, that for coarse discretisations, a significant increase in step size can be achieved.
Nevertheless, this approach also has some disadvantages. First, an easy ODE formulation $\dot u = f(t,u)$ is problematic, since the inverse of the mass-constraint matrix is full, so an $\mathcal{O}(N)$ multibody formalism [24, 55] has to be applied. As a second point, stabilisation of the constraints is not trivial and in general numerically more expensive as in the case of our discrete Cosserat model. The third disadvantage concerns

OPS	curv. (i)	curv. (ii)	curv. (iii)	curv. (iv)	curv. (v)	Baumgarte accel.
$+$	$174N$+34	$+11N$+11	$+11N$+10	$+10N$+10	$+37N$+37	$+8N$+00
$-$	$111N$+36	$+27N$+27	$+15N$+15	$+15N$+15	$+03N$+03	$+1N$+00
$*$	$289N$+90	$+36N$+36	$+40N$+39	$+39N$+39	$+72N$+72	$+2N$+00
$/$	$3N$+03	$+31N$+31	$+30N$+30	$+30N$+30	$+03N$+03	$+0N$+00
^{2}	$4N$+00	$+00N$+00	$+00N$+00	$+00N$+00	$+01N$+01	$+4N$+00
$\sqrt{}$	$0N$+00	$+01N$+01	$+00N$+00	$+00N$+00	$+01N$+01	$+0N$+00
arccos	$0N$+00	$+00N$+00	$+00N$+00	$+00N$+00	$+01N$+01	$+0N$+00

Table 1: *Upper estimates for the total number of operations for the Cosserat dynamic right-hand side function f in ODE form $(\dot{q}, \dot{v}) = f(q, v, t)$ for different curvature types.*

especially the inextensible Kirchhoff rod model, which theoretically allows for the largest step sizes due to the absence of all stiff dof: The mass-constraint matrix may become *singular* in certain configurations. This happens e. g. in the case of straight rod, which in applications is frequently chosen as the initial configuration! Therefore, additional inconvenient treatments are necessary in such a case.
As a consequence, concerning the treatment of the stiff extensional and shearing springs, we choose a different strategy, following another advice given in [60], according to which numerical difficulties may be alleviated by dissipation in the elastic model. Our numerical tests show that the full Cosserat rod model with consistent strong damping on tension and shearing performs significantly better than the (in)extensible Kirchhoff one, with the constraints introduced as sketched above.
However, a pure bending and torsion rod model of Kirchhoff type in quaternionic minimal coordinates will be the topic of further research. □

4 Numerical examples

In this section, we compare the solutions of our model to the solutions of finite element models, computed with ABAQUS, modeled both with 1D (shear flexible) beam and 3D continuum/brick elements. We further demonstrate the performance of our model for two simple scenarios with strong damping on the extensional and shearing dof.
For all four scenarios in this section, initially at $t = 0$, the rod is completely straight, not pre-deformed, aligned along the global e^2-axis and discretised equidistantly,

$$x_n(0) = \frac{n}{N} L e^2 \quad \text{for } n = 0, \dots, N, \qquad p_{n-1/2}(0) = \frac{1 - e^1 - e^2 - e^3}{2} \quad \text{for } n = 1, \dots, N.$$

Thus we have $d^1(0) = e^3$, $d^2(0) = e^1$, $d^3(0) = e^2$ at $t = 0$. In each of the four examples, the gravitational acceleration $g = 9.81\mathrm{m\,s^{-2}}$ is acting along the negative e^3-direction.

For the following two comparative tests against ABAQUS, we employed the discrete curvature type (ii), see section 3.1.

Test 1 vs. Abaqus (dynamic) In a first test, we compare a $L = 1.0$m long dynamically swinging pendulum rubber rod, subdivided into $N = 10$ segments, circular cross section with radius $r = 5.0\mathrm{E}^{-3}$m and end centroid $x_0(t) \equiv x_0 = 0$ fixed under gravity load with $g = 9.81\mathrm{ms}^{-2}$. Some snapshots of the scenario are depicted in Figure 3. The rubber material parameters are chosen as $E = 5.0\mathrm{E}^{+6}\mathrm{Nm}^{-2}$, $\nu = 0.5$, $G = E/2(1+\nu)$ and $\varrho = 1.1\mathrm{E}^{+3}\mathrm{kgm}^{-3}$. All the examples in this section have been performed with shear correction factors equal to $\kappa_1 = \kappa_2 = 1$.
Figure 4 shows fine agreement compared to the corresponding ABAQUS 1D solution, computed with B31 Timoshenko shear flexible beam elements. It is seen that not only the centroid and frame positions, but as well the forces and moments are reflected accurately. The same applies to the (angular) velocities and the (angular) accelerations, which are not plotted here.

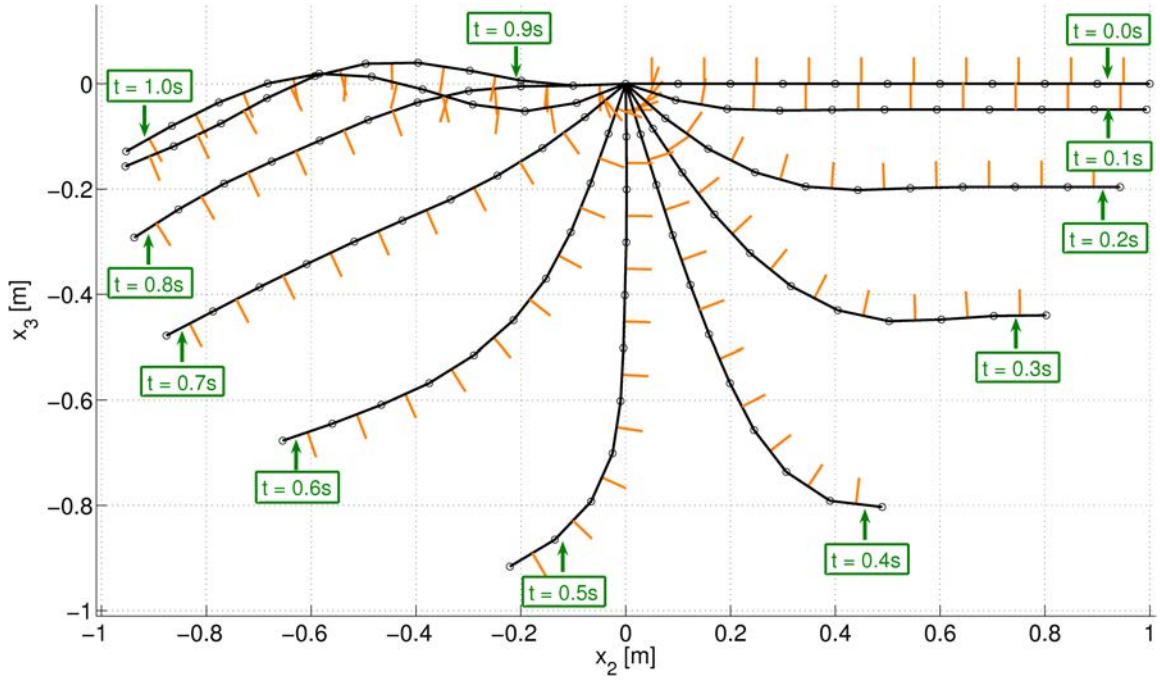

Figure 3: *Snapshots of the dynamic Test 1. (Plotted are the centerline centroids $x_n(t)$ and the first directors $d^1_{n-1/2}(t)$, which are — almost — perpendicular to the tangents $\Delta x_{n-1/2}(t)$. Note that $d^2_{n-1/2}(t) = e^1$ for all $t \in [0,T]$ and $n = 1, \ldots, N$.)*

Small differences in the solutions occur for the following reasons. An important one is that ABAQUS uses a discrete *curvature* that differs significantly from ours. Going into details would go beyond the scope of this article. Not only the curvature, but as well the continuous Cosserat *strain* Γ differs from the one that ABAQUS uses. In the Cosserat model, as seen from (5) and the orthonormality of the directors (d^1, d^2, d^3), shearing automatically induces negative extension. This means that, as soon as shearing $\Gamma^1 \neq 0$ or $\Gamma^2 \neq 0$ occurs, the rod must become slightly shorter in the longitudinal direction in order to make the extensional strain Γ^3 vanish. In contrast to that, shearing and extension are decoupled in ABAQUS. It uses

$$\Gamma^1_\bullet = \langle d^1, \partial_s x\rangle = \Gamma^1, \qquad \Gamma^2_\bullet = \langle d^2, \partial_s x\rangle = \Gamma^2, \qquad \Gamma^3_\bullet = \|\partial_s x\| - 1.$$

as a measure for the material strain instead of (5). Note that the coupling of shearing and extension in the Cosserat model is a second order effect in the shearing angle $\alpha = \arccos\langle d^3, \tau\rangle$ between the cross section normal d^3 and the centerline unit tangent $\tau = \partial_s x/\|\partial_s x\|$, as $\Gamma^3 = \langle \tau, \partial_s x\rangle + \langle d^3 - \tau, \partial_s x\rangle - 1 = \langle \tau, \partial_s x\rangle - 1 + \|\partial_s x\|(\cos\alpha - 1) = \Gamma^3_\bullet + \mathcal{O}(\alpha^2)$ holds. For the classical Kirchhoff rod models, the measures $\Gamma^3_\bullet$ and Γ_3 coincide, since $\Gamma^1 = \Gamma^2 = 0$, cf. remark 2.1.
These differences in the models cause the solutions of both models to diverge with increasing time, especially in the undamped case, see Figure 4.
Since the system is undamped, we used the explicit method DOPRI5 with ABSTOL= RELTOL= 1.0E^{-8} for time integration in this test. In order to avoid the drift-off, we used the projection method. DOPRI5 needed amounts of time steps and right-hand side function calls that are similar to ones presented in Table 2. Note that, here in the undamped case, DOPRI5 is more efficient than the implicit methods we have tested, whereas it fails in the case of strongly damped shearing and extension, see the performance tests below.

Test 2 vs. Abaqus (quasistatic) In a second test, we compare the quality of our discretisation scheme with the full 3D ABAQUS solution. To that end, a 3D continuum FE model of the rubber rod

Figure 4: *Dynamical comparison with* ABAQUS *1D finite element solution (Test 1). Plotted are* $x_2(t)$, $x_3(t)$, $d_3^1(t) = \langle e^3, d^1(t)\rangle$, $M^2(t) = EI_2K^2(t)$, $F^1(t) = GA_1\Gamma^1(t)$, $F^3(t) = EA\Gamma^3(t)$ *according to (16).*

of Test 1 has been set up in ABAQUS. It is discretised with 160 (in longitudinal direction) × 12 (in the cross section) continuum/brick elements of type C3D8; in total, these are 1920 elements. We consider the scenario that is plotted in Figure 5. It includes a non-trivial coupling of bending and torsion. The fully clamped boundary conditions $(x_0(t), p_0(t))$ and $(x_N(t), p_N(t))$ are chosen in the way that the rod traverses the shape of the Greek letter 'γ' (front view) or the Greek letter 'Ω' (side view).
To be more precisely, we push the boundary centroids together along the e^2-axis,

$$x_0(t) = \frac{L}{2} t e^2, \qquad x_N(t) = L\Big(1 - \frac{t}{2}\Big) e^2,$$

and turn around the boundary quaternions

$$p_0(t) = \wp\Big(t, \frac{1 - e^1 - e^2 - e^3}{2}, \frac{1 - e^1 + e^2 + e^3}{2}\Big), \quad p_N(t) = \wp\Big(t, \frac{1 - e^1 - e^2 - e^3}{2}, -\frac{1 - e^1 + e^2 + e^3}{2}\Big),$$

by an angle of $\pi/2$. Here the function

$$\wp(t, q_0, q_1) = \frac{1}{\sin\theta}\Big(\sin\big((1-t)\theta\big) q_0 + \sin(t\theta) q_1 \Big), \qquad \theta = \arccos\langle q_0, q_1 \rangle$$

interpolates $q_0,\ q_1 \in \mathbb{S}^3$, such that $q_0 \neq -q_1$, spherically linearly in the interval $t \in [0,1]$. In this example, $t \in [0,1]$ is a non-dimensional, fictive time, which we prefer to call 'pseudotime'. Note that the boundary frames $R(p_0(t))$ resp. $R(p_N(t))$ turn around the e^2-axis by an angle of π resp. $-\pi$ and that $R(p_0(1)) = R(p_N(1))$ for $t = 1$, since $p_0(1) = -p_N(1)$.
Figure 6 shows fine agreement of the results of our discrete Cosserat model. The results are competitive to the results obtained by ABAQUS shear flexible beam elements B31, see Figure 6. We emphasise that for our discrete Cosserat rod model, we took only $N = 10$ segments. Numerical experiments indicate that the proposed discretisation is a second order approximation of the continuous equations (20) in the equidistant case [38].
These results as well confirm that the Cosserat rod theory is an excellent approximation to the full three-dimensional theory. Clearly, the thinner the rod, the better the agreement with the 3D solution. Interestingly, the centerline of the 3D solution at $t = 1$ — after self-intersection — for this scenario lies in the plane $\{x : x_1 = 0\}$, see Figure 5. So does ours, in contrast to the ABAQUS B31 beam solution. See the results for the x_1-displacement at $t = 1$ in Figure 6.

Let us finally give some comments, how we solved the quasistatic problem. The quasistatic balance equations of forces and moments are obtained from the dynamical ones (21) by letting $\ddot{q} = \dot{v} = 0$, $\dot{q} = v = 0$, yielding

$$\left\{ \begin{array}{rcl} 0 & = & \mathcal{F}(q,t) - \mathcal{G}(q)^\top \lambda \\ 0 & = & g(q) \end{array} \right. \tag{31}$$

with the right hand side forces $\mathcal{F}(q,t) = \hat{\mathcal{F}}(t) - \partial_q \mathcal{V}(q,t)$. We solved this problem, as it is standard in nonlinear incremental elastostatics, see e. g. [46] for the unconstrained case. The incremental form of (31) is obtained by time differentiation with respect to the pseudotime t,

$$\begin{pmatrix} \dot{q} \\ \dot{\lambda} \end{pmatrix} = \begin{pmatrix} \partial^2_{qq} \mathcal{V}(q,t) + \partial^2_{qq} g[\cdot, \lambda] & \mathcal{G}(q)^\top \\ \mathcal{G}(q) & 0 \end{pmatrix}^{-1} \begin{pmatrix} \partial_t \mathcal{F}(q,t) \\ 0 \end{pmatrix}. \tag{32}$$

This can be interpreted as the index reduced version — the underlying ODE — of the index one (D)AE (31). The inverse of the matrix in (32) constitutes the stiffness-constraint matrix of the system.
In our example, 25 equidistant pseudotime steps (= 'increments') along $[0,1]$ were sufficient to solve the problem. In each step, we applied an explicit Euler step from (32) as a predictor, followed by a full Newton iteration to project the solution back onto the constraint manifold, which is given by (31). Typically about 4 to 6 corrector iterations were sufficient to have the balance of forces and moments (31) satisfied up to roundoff errors. However, we did not focus on a good or an even optimal numerical scheme for quasistatics, including e. g. automatic pseudotime stepsize selection.

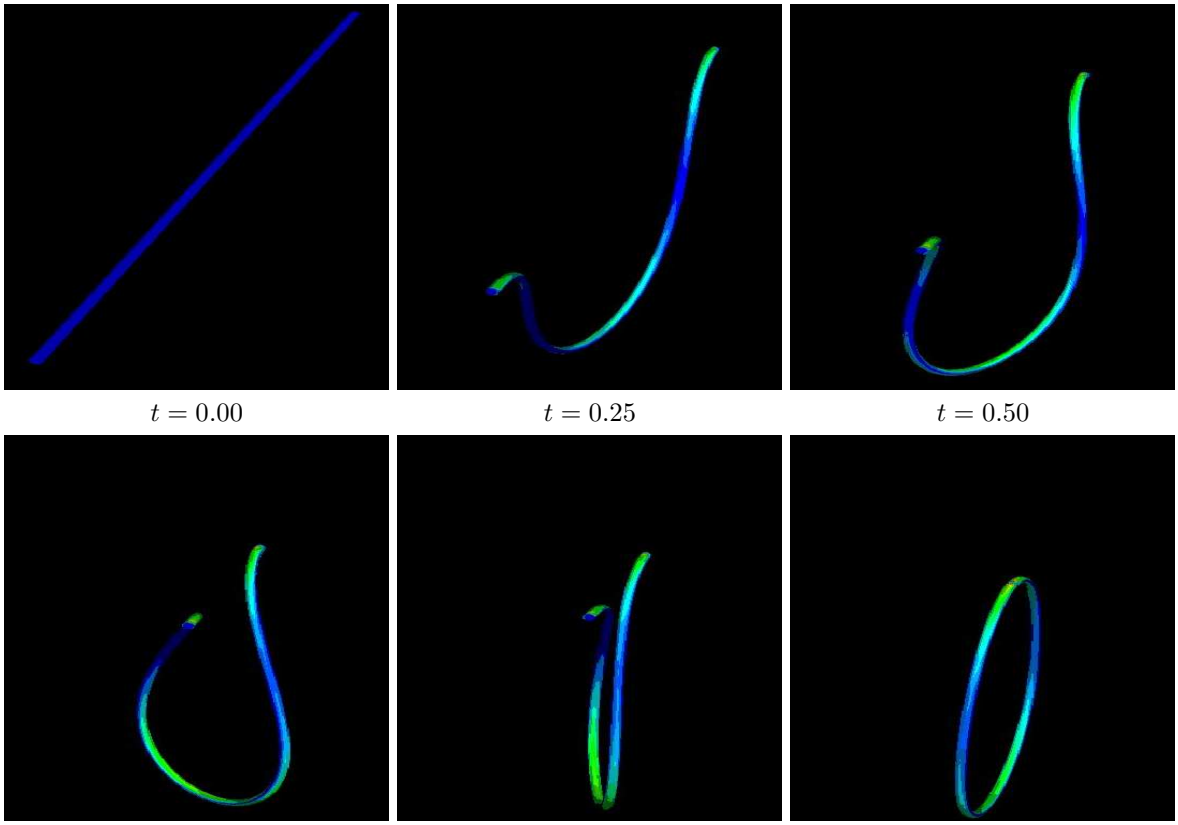

Figure 5: *Snapshots of the quasistatic Test 2. (Colored is the Mises stress.)*

Two performance examples. Now we introduce some damping into the model, slight damping for bending and torsion, $c_1^{\dot{K}} = c_2^{\dot{K}} = 2.0\text{E}^{-4}\text{kg m}^3$, $c_3^{\dot{K}} = 8.0\text{E}^{-6}\text{kg m}^3$, and strong damping for shearing and extension, $c_1^{\dot{\Gamma}} = c_2^{\dot{\Gamma}} = 1.0\text{E}^{-1}\text{kg m}$, $c_3^{\dot{\Gamma}} = 2.0\text{E}^{+2}\text{kg m}$. As we apply the multistep solver DASPK amongst others, we prefer the Baumgarte to the projection stabilisation technique. For the Baumgarte parameters, we choose $\omega = r = 1.0\text{E}^2\text{s}^{-1}$, thus the constraint defect is critically damped without introducing significant additional stiffness into the model.

For a *rubber example*, we choose the same swinging pendulum with fixed end centroid $x_0(t) \equiv x_0 = 0$ as in the comparative Test 1 vs. ABAQUS above. For a *steel string example*, we choose a string of length $L = 1.0\text{m}$ and radius $1.0\text{E}^{-3}\text{m}$ without precurvature, clamp in fully at $s = 0$, i. e. $x_0(t) \equiv x_0 = 0$ and $p_0(t) \equiv p_0 = (1 - e^1 - e^2 - e^3)/2$, and subject it to gravity load. The material parameters for steel are set to $E = 2.1\text{E}^{+11}\text{Nm}^{-2}$, $\nu = 0.2$, $G = E/2(1+\nu)$ and $\varrho = 7.85\text{E}^{+3}\text{kg m}^{-3}$.

In both cases, the parameters are chosen such that shearing and extension oscillations are damped out more than critically. This means that the eigenvalues of the Jacobian $\partial f(u)/\partial u$, $u = (q, v)$, — i. e. the eigenfrequencies of the straight linearised rod — that are corresponding to the shearing and extensional eigenmodes do lie on the negative real axis $\{z \in \mathbb{C} : \Re(z) < 0,\ \Im(z) = 0\}$. Bending is just slightly damped, as can be seen from the evolution of rod extreme in Figure 9. The eigenvalues of $\partial f(u)/\partial u$ corresponding to bending and torsion lie in the half-plane $\{z \in \mathbb{C} : \Re(z) < 0\}$, but they are close to the imaginary axis.

In both performance examples, we used curvature (iii), which is highly robust, but still cheap to evaluate. In both examples, the number of unknowns in q is equal to 70.

Figure 9 displays the reference solutions of the rod extremes — the free end at $n = N$ — obtained with the integrator RADAU5 with tolerances ABSTOL= RELTOL= 1.0E^{-10}. Let $d_j^i(t) = \langle e^j, d^i(t)\rangle$ for

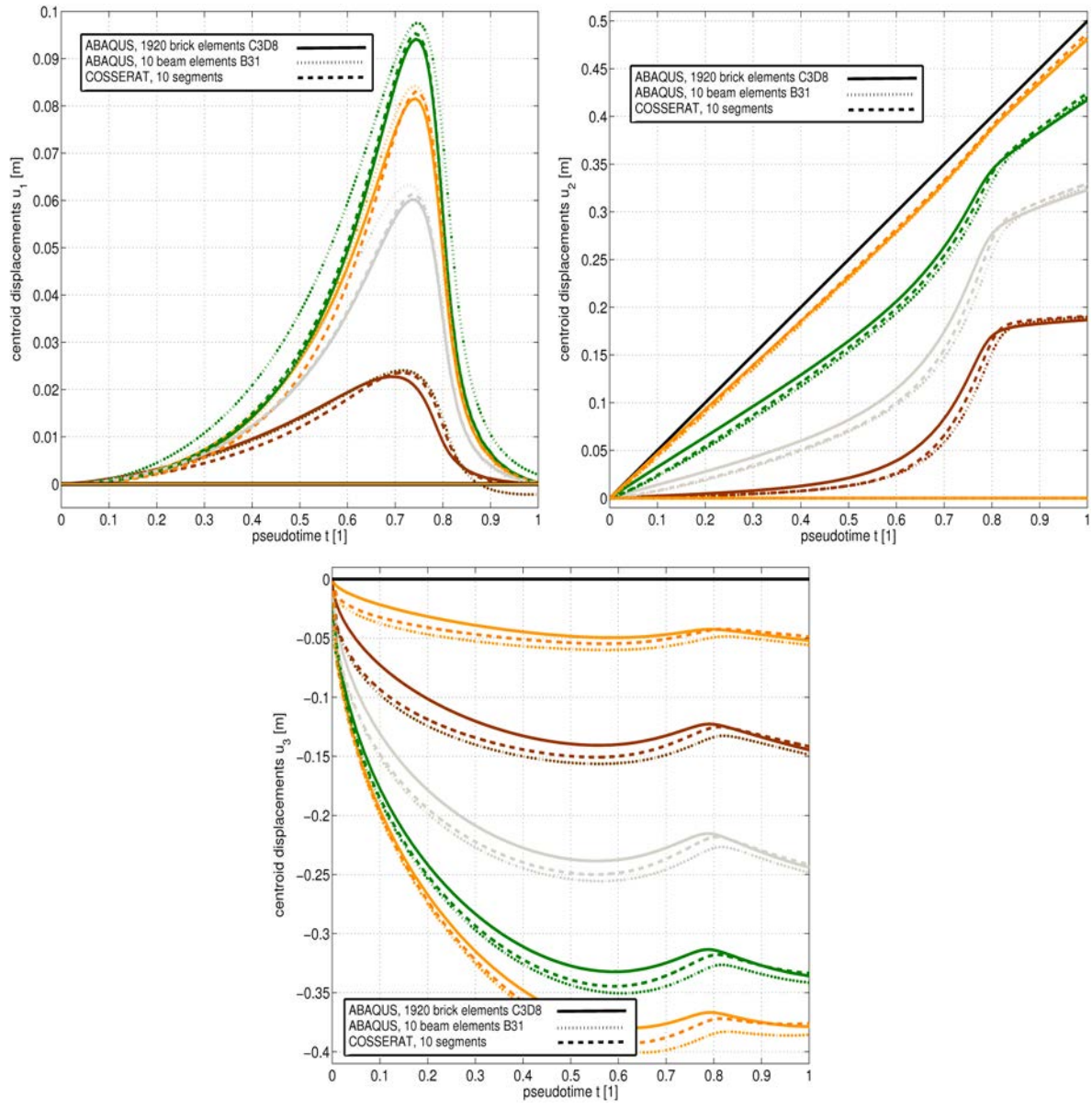

Figure 6: *Quasistatic comparison with* ABAQUS *3D finite element solution (Test 2). Plotted are the centerline displacements that are corresponding to the centroids* $x_0(t), \ldots, x_5(t)$ *at the vertex positions* $s_0, \ldots, s_5$. *(Note that the solution is symmetric w.r.t. the midpoint of the rod throughout the deformation, since the initial and boundary values are symmetric.)*

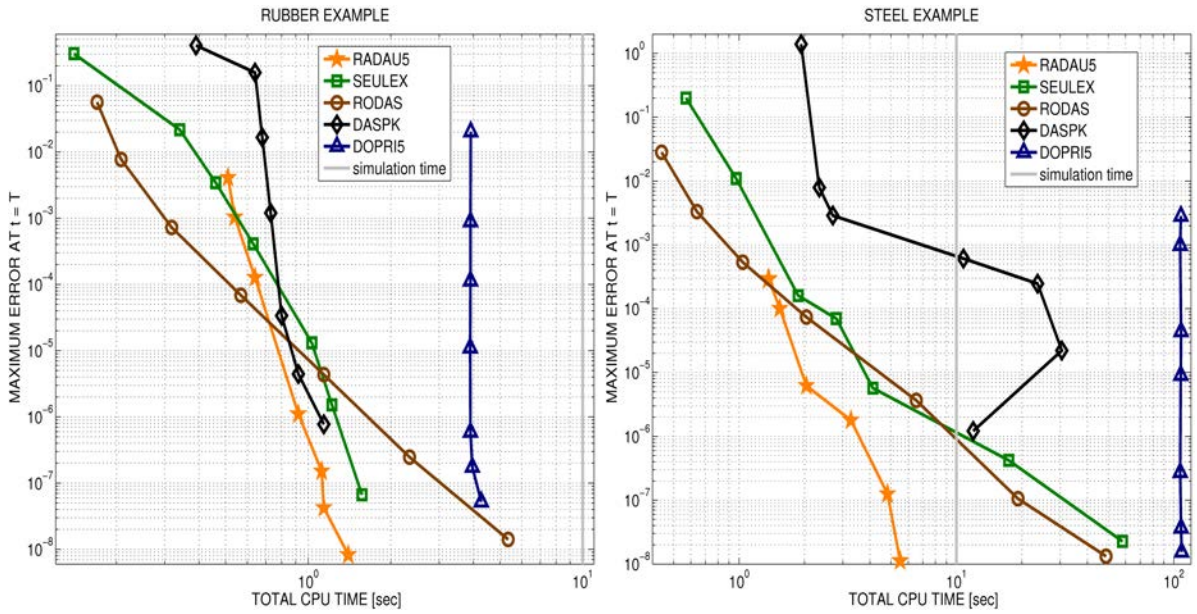

Figure 7: *Computational times and accuracies for different solvers. (The markers correspond to integrator tolerances* TOL= RELTOL= ABSTOL= 1.0E^{-2}, ..., 1.0E^{-8}, cf. as well the corresponding solver statistics in Tables 2 and 3.)

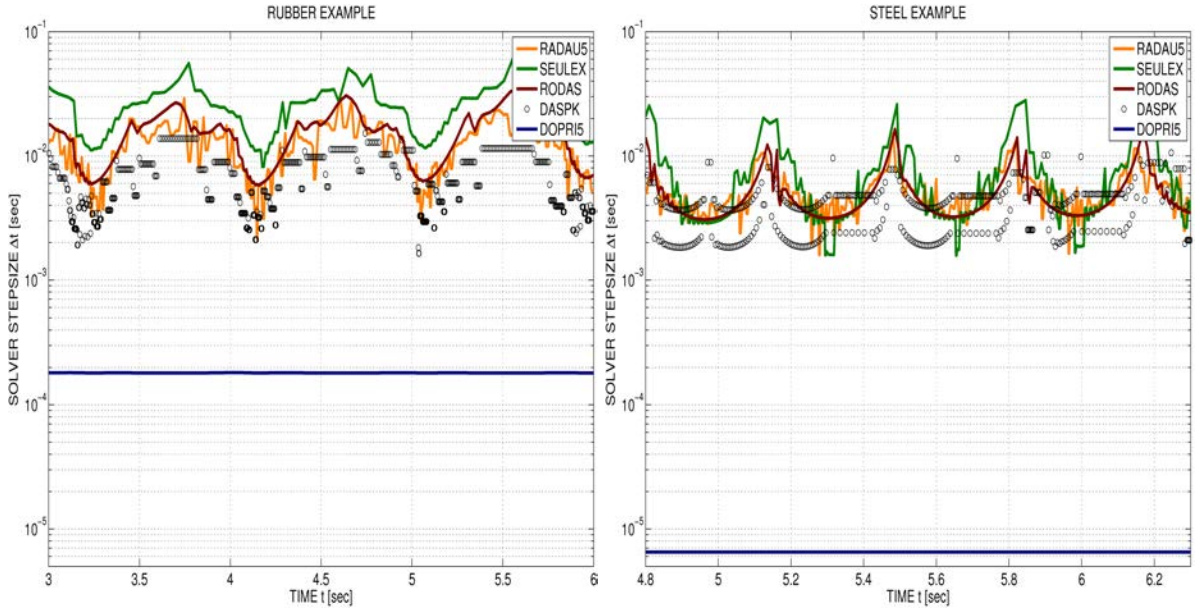

Figure 8: *Step size behaviour for different solvers. (*ABSTOL= RELTOL= 1.0E^{-3}*)*

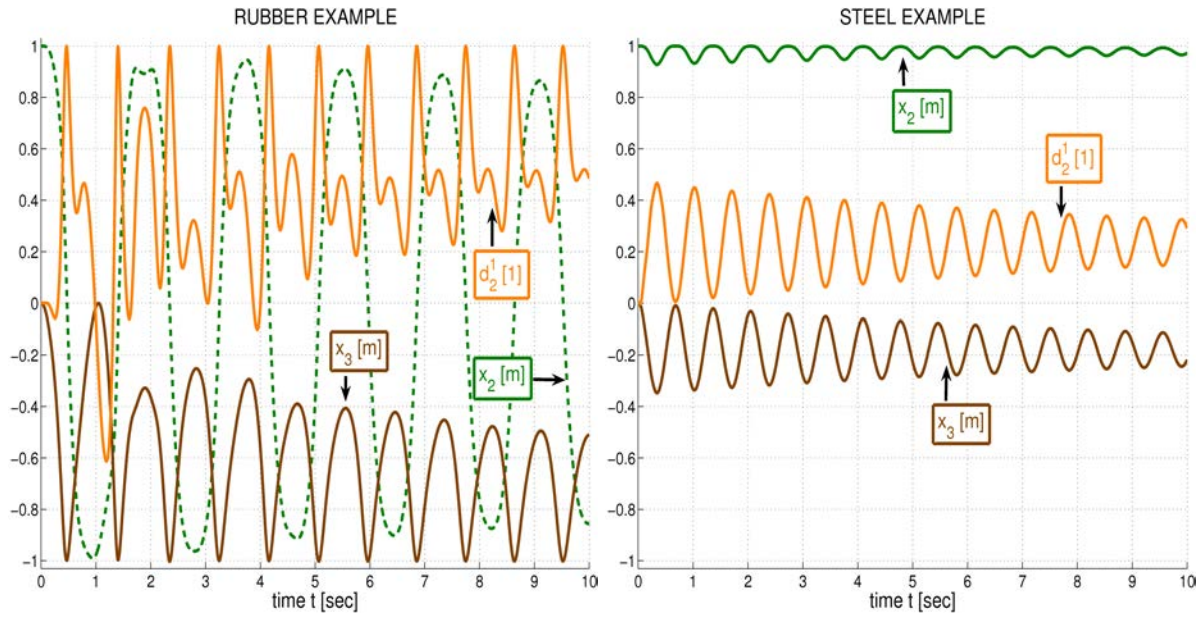

Figure 9: *The reference solution at the rod extremes at* $n = N = 10$. *Here* $d_2^1(t) = \langle e^2, d^1(t)\rangle$ *denotes the* e^2*-component of the director* $d^1(t)$.

Tol		Radau5	Seulex	Rodas	Daspk	DoPri5
10^{-2}	# f	12 089	2 725	4 050	1 408	331 610
	# $\partial f/\partial u$	821	335	600	319	0
	# steps	1 645	453	688	478	55 268
10^{-3}	# f	12 555	8 882	4 764	3 358	331 610
	# $\partial f/\partial u$	877	433	769	458	0
	# steps	1 714	584	799	1 508	55 268
10^{-4}	# f	14 679	14 066	7 242	4 403	331 622
	# $\partial f/\partial u$	1 071	463	1 202	427	0
	# steps	2 050	487	1 208	2 299	55 270
10^{-5}	# f	21 187	22 311	12 990	6 075	331 694
	# $\partial f/\partial u$	1 507	443	2 165	437	0
	# steps	2 910	473	2 165	3 263	55 282
10^{-6}	# f	26 285	38 742	25 440	7 301	332 228
	# $\partial f/\partial u$	1 809	551	4 240	438	0
	# steps	3 354	628	4 240	3 948	55 371
10^{-7}	# f	27 463	46 864	54 588	9 659	337 184
	# $\partial f/\partial u$	2 020	654	9 098	443	0
	# steps	3 224	659	9 098	5 551	56 179
10^{-8}	# f	33 829	59 751	125 382	12 952	364 376
	# $\partial f/\partial u$	2 584	895	20 897	471	0
	# steps	3 813	899	20 897	7 703	60 729

Table 2: *Solver statistics for rubber rod performance example. (Here* $T = 10s$*).*

TOL		RADAU5	SEULEX	RODAS	DASPK	DOPRI5
10^{-2}	# f	30 804	11 450	10 423	6 810	9 211 232
	# $\partial f/\partial u$	2 096	1 539	1 568	1 670	0
	# steps	4 210	2 667	1 771	1 865	1 535 205
10^{-3}	# f	31 355	19 073	15 040	6 450	9 211 244
	# $\partial f/\partial u$	2 146	2 136	2 430	1 973	0
	# steps	4 323	3 062	2 522	1 697	1 535 207
10^{-4}	# f	35 087	39 904	24 183	10 019	9 211 256
	# $\partial f/\partial u$	2 296	3 669	3 963	2 544	0
	# steps	5 007	4 190	4 044	3 499	1 535 209
10^{-5}	# f	44 426	77 994	47 438	30 288	9 211 268
	# $\partial f/\partial u$	2 985	3 374	7 848	9 144	0
	# steps	6 715	4 428	2 918	11 417	1 535 211
10^{-6}	# f	74 581	127 326	153 475	81 948	9 211 298
	# $\partial f/\partial u$	4 218	4 247	25 525	33 502	0
	# steps	12 075	4 342	25 590	26 983	1 535 216
10^{-7}	# f	107 035	533 384	449 887	69 220	9 211 304
	# $\partial f/\partial u$	6 915	17 868	74 862	20 244	0
	# steps	15 972	18 010	75 005	31 517	1 535 217
10^{-8}	# f	129 280	1 720 395	1 146 392	138 874	9 211 310
	# $\partial f/\partial u$	7 853	57 654	190 917	5 961	0
	# steps	17 272	57 780	191 095	98 652	1 535 218

Table 3: *Solver statistics for steel string performance example. (Here $T = 10s$).*

$i, j = 1, 2, 3$ denote the jth component of the ith director w. r. t. the global system (e^1, e^2, e^3). Since both examples are plane scenarios, we have $d^2(t) \equiv e^1$, $d_1^1(t) \equiv d_1^3(t) \equiv 0$ and $x_1(t) \equiv 0$ in both cases. Thus, from the information given in Figure 9 and the orthonormality of the directors, the complete solution — the centroid $x(t)$ and the frame $R(t) = (d^1(t), d^2(t), d^3(t))$ — can be easily reconstructed.

Figure 7 shows the computational times for the solvers RADAU5 (an implicit Runge-Kutta method), SEULEX (an extrapolation method), RODAS (a Rosenbrock method), DOPRI5 (an explicit Runge-Kutta method) from [27, 28, 29, 43] and DASPK (= DASSL, a multistep BDF method) from [49] at several tolerances. For all the computations we choose TOL= ABSTOL= RELTOL, discarding the error control for the Lagrange multipliers. Clearly, the problem is stiff even for rubber material because of the presence of the high extensional and shearing frequencies [38]. Thus, DOPRI5 fails, the corresponding step sizes in Figure 8 indicate that it runs at the stability limit. In contrast to that, the four stiff solvers reveal satisfactory step size behaviour. We remark that Figure 8 displays just an excerpt of the time step histories for the five solvers. Clearly, the mean time step sizes of the implicit integrators increase *slightly* along $[0, T]$, since the internal total energy is dissipated slightly with time. For RADAU5, we did not discover any significant difference between the classical and the Gustafsson step size strategy.

For the solvers RADAU5, SEULEX and RODAS, we chose sparse linear algebra, adapted to second order ODEs, with upper resp. lower bandwidths MUJAC resp. MLJAC of the Jacobians $\partial f/\partial q$ and $\partial f/\partial v$ equal to ten. RADAU5 spent about 38% of the total computational time in order to evaluate f and $\partial f/\partial u$, SEULEX about 43% and RODAS about 61%. The remaining percentage is needed for (non)linear algebra. Roughly, an evaluation of f needs about 1.06E^{-5}s, which is comparable to [63], but with a much more robust curvature model, an evaluation of $\partial f/\partial u$ needs about 1.02E^{-4}s, this is about ten times larger.

Clearly, for coarse discretisations and rough error control during time integration, RODAS performs best. Here, for the rubber pendulum example, the factor to the real physical time is 47, for the steel string example 17. The results that are obtained for coarse tolerances ABSTOL= RELTOL= 1.0E^{-2} are still accurate enough for virtual reality applications such as industrial path planning, the modeling of cables and hoses. For more stringent tolerances and high accuracy demands, RADAU5 performs best, since it is a high order method.

The computations have been performed on a 2.19 GHz Dual Core AMD (Opteron) machine on one CPU and on one core. For further discussions of special numerical topics in time integration for classical Cosserat and Kirchhoff rods, we refer to [38].

5 Conclusions

We presented a numerically stable and efficient method for the dynamical analysis of Cosserat rods that computes within milliseconds numerical results with an accuracy similar to detailed finite element solutions. At its heart, this novel approach is based on a coarse grid finite difference approximation that follows from a discrete variational principle taking into account the overall requirement of frame-indifference and considering the material damping by Rayleigh damping terms. A consistent semi-discretisation of the continuous dynamical Cosserat partial differential equations of motion is achieved combining two staggered space grids. From the algorithmic viewpoint, the parametrisation of rotations by quaternions proved to be very useful. For time integration, standard ODE and DAE solvers were applied.
All basic components of this approach are not restricted to Cosserat rods and may be extended to plate and shell structures. Further gains in efficiency may be expected from the use of null-space methods in time integration that are tailored to quaternion representations of the rotational degrees of freedom. The incorporation of geometrical constraints like obstacles in the model is especially interesting from the viewpoint of practical application but yields fundamentally new problems in theory, in space discretisation and in the final full (space-time) integration of the equations of motion. A reference implementation of the proposed approach in a virtual reality tool for vehicle design is under development.

A Objective finite difference approximations of curvature

The numerical evaluation of the potential energy (24) as well as the symbolic computation of its various gradient terms appearing on the r.h.s. of the discrete balance equations (29) requires explicit algebraic expressions of the discrete curvatures as generally defined by the finite difference ansatz (25) in terms of the adjacent midpoint quaternions $p_{n\pm1/2}$. In the following we present several possible choices of the vertex quaternion p_n and the corresponding expression δp_n which explicitly lead to the FD approximations (26) of the discrete vertex curvature via the finite difference ansatz (25), including a geometrical interpretation of these expressions via trigonometry and spherical geometry. Recall that $\delta s_n = s_{n+1/2} - s_{n-1/2}$ in the sequel. Each ansatz is illustrated in Figure 10.

(i) The simplest variant (see e. g. [63]) is obtained by using the secant $\delta p_n = p_{n+1/2} - p_{n-1/2}$ and linear midpoint interpolation $p_n = (p_{n-1/2} + p_{n+1/2})/2$, regardless of the fact that this choice of p_n violates the condition of unit length, and results in $\zeta(\theta) = 1$. This choice leads to a 'soft' behaviour of the curvature with an increasing size of the relative rotation angle between frames, which results in poor stability properties for large bending or torsion angles, as we shall see. Phenomena such as 'quaternion flipping' (= sign change) might be the consequence.

(ii) Here we choose $p_n = (p_{n-1/2} + p_{n+1/2})/(2 + 2\langle p_{n-1/2}, p_{n+1/2}\rangle)^{1/2}$, which is the midpoint of the great circle that is joining $p_{n-1/2}$ to $p_{n+1/2}$, and the secant $\delta p_n = p_{n+1/2} - p_{n-1/2}$. Note that p_n is in $\mathbb{S}^3$, if $p_{n-1/2}$ and $p_{n+1/2}$ are so. Using the identity $\|p+q\|^2 = 2 + 2\langle p, q\rangle$ for $p, q \in \mathbb{S}^3$, this choice leads to $\zeta(\theta) = \sqrt{2/(1+\cos\theta)}$.

(iii) The third variant, which is identical to the one discussed in [33] and generalises the definitions of the discrete vertex bending curvature proposed in [8, 12] for inextensible Kirchhoff rods, may be obtained by choosing either $p_n = p_{n-1/2}$ combined with a tangential forward difference $\delta p_n = p_{n+1/2}/\cos\theta_n - p_{n-1/2}$, or $p_n = p_{n+1/2}$ combined with a tangential backward difference $\delta p_n = p_{n+1/2} - p_{n-1/2}/\cos\theta_n$ — or the arithmetic mean of both. Straightforward algebra shows that each of these choices leads to $K_n \delta s_n = 2\Im(W_n)/\Re(W_n)$, which corresponds to $\zeta(\theta) = 1/\cos(\theta)$. Interesting properties of this curvature approximation are its 'flip invariance' as well as the singularity — yielding infinite bending and torsional stiffness — at $\theta_n \to \pi/2$, which prevents the occurrence of degenerate configurations at finite deformation energy. (See also [33] for a discussion.)

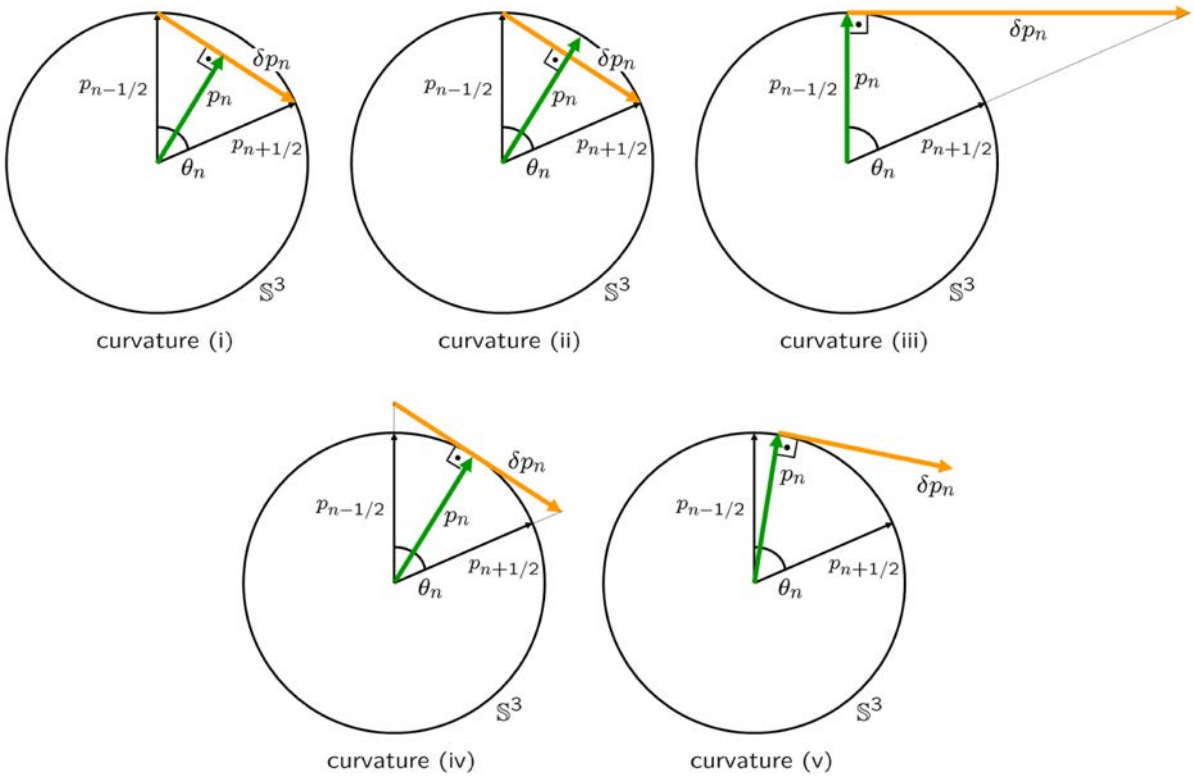

Figure 10: *Geometric illustration of the interpolation and finite difference ansatzes used in the discrete approximations of the vertex curvature* K_n

(iv) To obtain the fourth variant, we use p_n as in (ii), combined with the tangential central difference $\delta p_n = (p_{n+1/2} - p_{n-1/2})/\cos(\theta_n/2)$. Similarly to (iii), curvature (iv) displays a stiffening behaviour at increasing angles, with a singularity (corresponding to infinite stiffness) occurring at $\theta_n \to \pi$, i. e. at an angle twice as large as for (iii).

(v) We obtain this last variant on the basis of a *geodesic interpolation* connecting the pair of unit quaternions $p_{n-1/2}$ and $p_{n+1/2}$, assumed to be non-antipodal (i. e. $p_{n+1/2} \neq -p_{n-1/2}$), on the great circle arc parametrised by the spherically linear interpolating function [59]

$$\wp(s) = \frac{1}{\sin\theta_n}\Big(\sin\big((1-\sigma)\theta_n\big)p_{n-1/2} + \sin\big(\sigma\theta_n\big)p_{n+1/2}\Big)\Big|_{\sigma=(s-s_{n-1/2})/\delta s_n}. \tag{33}$$

An evaluation of the product $\bar{\wp}(s)\partial_s\wp(s)$ at any curve parameter $s \in [s_{n-1/2}, s_{n+1/2}]$ reveals the well known fact that $\bar{\wp}(s)\partial_s\wp(s)$ is completely *independent* of s and depends solely on the endpoints $p_{n-1/2}$ and $p_{n+1/2}$, see [20, 59]. This variant, resulting in the expression $\zeta(\theta)$ in (v), is thus applicable without modification in the case of a non-equidistant discretisation as well. Recently this variant was applied as special case within the so-called 'geodesic finite element' approach proposed by [53], where it appears naturally due to the fact that the great circle arcs (33) are the geodesic lines in the manifold / sphere $\mathbb{S}^3$ [59].

Let us translate the five proposed discrete curvature measures from the quaternionic into the setting of rotations in Euclidean space. To that end, we rewrite the material quotient/difference quaternion W_n in the form $W_n = \cos(\phi_n/2) + \sin(\phi_n/2)u_n$ with a purely imaginary (= vector) unit quaternion $u_n \in \mathbb{S}^3 \cap \Im(\mathbb{H})$, which represents the material unit axis of rotation, and the Euclidean difference angle

ϕ_n, which is precisely *twice* the quaternionic difference angle θ_n [23, 25], i. e. $\phi_n = 2\theta_n$. Then, it is straightforward to see that the five proposed curvature measures correspond to

$$\text{(i)}\ K_n = \frac{2}{\delta s_n}\sin\Big(\frac{\phi_n}{2}\Big)u_n, \qquad \text{(ii)}\ K_n = \frac{4}{\delta s_n}\sin\Big(\frac{\phi_n}{4}\Big)u_n, \qquad \text{(iii)}\ K_n = \frac{2}{\delta s_n}\tan\Big(\frac{\phi_n}{2}\Big)u_n,$$

$$\text{(iv)}\ K_n = \frac{4}{\delta s_n}\tan\Big(\frac{\phi_n}{4}\Big)u_n, \qquad \text{(v)}\ K_n = \frac{\phi_n}{\delta s_n}u_n$$

in the Euclidean representation. It is worth mentioning that the families of Euclidean characteristic generating functions

$$\eta(\phi) = m\sin\Big(\frac{\phi}{m}\Big), \qquad \eta(\phi) = m\tan\Big(\frac{\phi}{m}\Big), \qquad \eta(\phi) = \phi \tag{34}$$

with any integer – or even real – parameter $m \geq 1$ all satisfy the conditions $\eta(0) = 0$ and $\eta'(0) = 1$, which are essential for the consistency of our finite difference schemes for small bending and torsion angles ϕ_n. The functions $\eta(\phi)$ all are strictly increasing on the interval $[0, \phi^*)$, where

$$\text{(i)}\ \phi^* = \pi, \qquad \text{(ii)}\ \phi^* = 2\pi, \qquad \text{(iii)}\ \phi^* = \pi, \qquad \text{(iv)}\ \phi^* = 2\pi, \qquad \text{(v)}\ \phi^* = \infty.$$

The tangent generators $\eta(\phi)$ of curvatures (iii) and (iv) even become singular at ϕ^*, i. e. $\eta(\phi) \to \infty$ for $\phi \to \phi^*$. Note that these singularities, yielding infinite bending and torsional stiffnesses at ϕ^*, are not the result of a hyperelastic constitutive material law — we use a linear one — but are caused by different geometric approaches in the spatial discretisation. Figure 11 displays the sine and tangent generators (34) for the cases $m = 2, 4, \infty$ corresponding to our discrete curvatures (i) to (v).
Curvature (v) can be considered as the limit case of both the sine and tangent generator family for $m \to \infty$. Concerning its quaternionic characteristic $\zeta(\theta) = \theta/\sin\theta$, one should remark that the composition $w \mapsto (\zeta \circ \arccos)(w) = \arccos(w)/\sqrt{1-w^2}$ is clearly analytical and especially admits Taylor expansion in a neighbourhood of $w = 1$, which corresponds to $p_{n-1/2} = p_{n+1/2}$.
The suggested curvature measures all differ in algebraic complexity (see Table 1) and numerical robustness (e. g. desired singularities for $\phi \to \phi^\star$). However, from the analytical viewpoint, it is not yet clear, which of them is 'the best'. Asymptotically for $|\phi| \ll 1$, they all coincide, see Figure 11.

References

[1] **Antman S. S.:** Kirchhoff's problem for nonlinearly elastic rods. *Quarterly of applied mathematics*, **32**, 221–240, 1974.

[2] **Antman S. S.:** Dynamical problems for geometrically exact theories of nonlinearly viscoelastic rods. *Journal of nonlinear science*, **6**, 1–18, 1996.

[3] **Antman S. S.:** *Nonlinear problems of elasticity*. Springer, 2005.

[4] **Arnold M.:** Numerical methods for simulation in applied mechanics. In: Simulation techniques for applied mechanics (Eds: Arnold M., Schiehlen W.), Springer, 191–246, 2008.

[5] **Bauchau O. A., Epple A., Bottasso C. L.:** *Scaling of constraints and augmented Lagrangian formulations in multibody dynamics simulations.* Journal of computational and nonlinear dynamics, **4** (2), 2009.

[6] **Bauchau O. A., Trainelli L.:** The vectorial parametrization of rotation. *Nonlinear dynamics*, **32** (1), 71–92, 2003.

[7] **Bauchau O. A., Epple A., Heo S.:** *Interpolation of finite rotations in flexible multi–body dynamics simulations. Proceedings of the institution of mechanical engineers*, **222** (4) Part K: Multi-body dynamics, 353–366, 2008.

[8] **Bergou M., Wardetzky M., Robinson S., Audoly B., Grinspun E.:** Discrete elastic rods. *ACM transaction on graphics*, **27** (3), 63:1–63:12, 2008.

[9] **Betsch P., Siebert R.:** Rigid body dynamics in terms of quaternions: Hamiltonian formulation and conserving numerical integration. *International journal for numerical methods in engineering*, **79** (4), 444–473, 2009.

[10] **Betsch P., Steinmann P.:** A DAE approach to flexible multibody dynamics. *Multibody system dynamics*, **8**, 365–389, 2002.

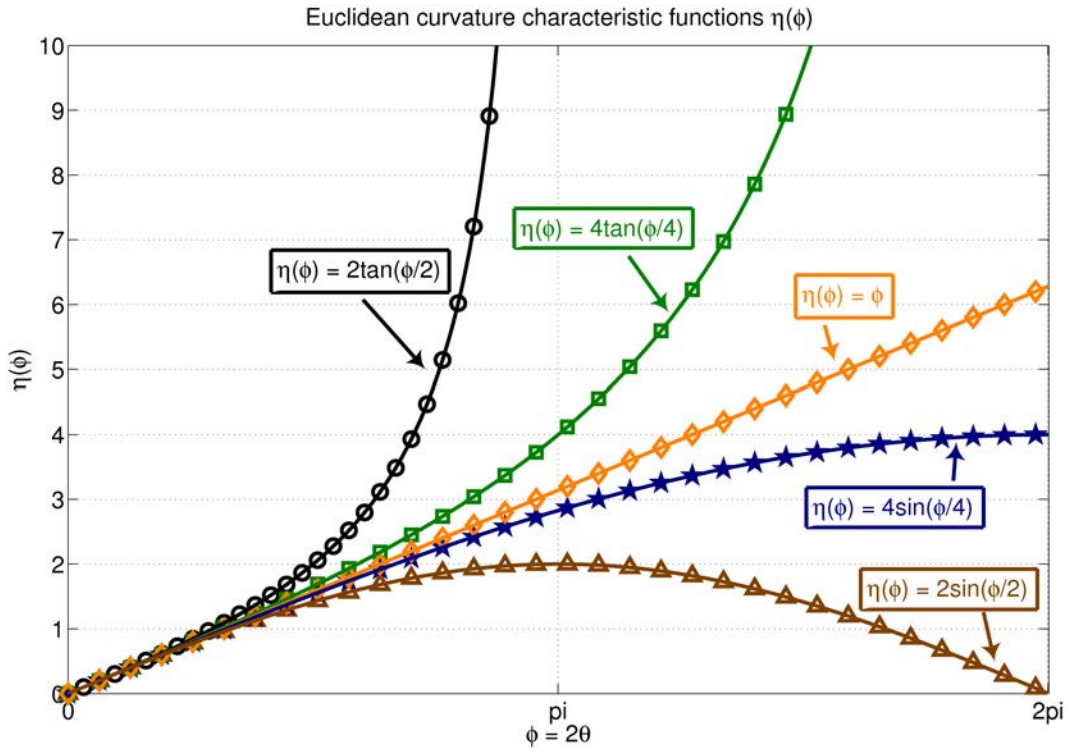

Figure 11: *Euclidean characteristic generating functions $\eta(\phi)$ of curvature corresponding to the sin– and tan–family of vectorial rotation parametrisations [6] in the cases $m = 2, 4, \infty$.*

[11] **Betsch P., Steinmann P.:** Frame-indifferent beam finite elements based upon the geometrically exact beam theory. *International journal for numerical methods in engineering*, **54**, 1755–1788, 2002.

[12] **Bobenko A. I., Suris Y. B.:** Discrete time Lagrangian mechanics on Lie groups with an application to the Lagrange top. *Communications in mathematical physics*, **204**, 147–188, 1999.

[13] **Cardona A., Géradin M.:** A beam finite element nonlinear theory with finite rotations. *International journal for numerical methods in engineering*, **26**, 2403–2434, 1998.

[14] **Cardona A., Géradin M.:** *Flexible multibody dynamics. A finite element approach.* Wiley, 2001.

[15] **Cartan H.:** *Differential Forms*, Kershaw Publishing, 1971, reprinted by Dover, 2006.

[16] **Chouaieb N., Maddocks J. H.:** Kirchhoff's problem of helical equilibria of uniform rods, *Journal of elasticity*, **77**, 221–247, 2004.

[17] **Cowper G. R.:** The shear coefficient in Timoshenko's beam theory. *Journal of applied mechanics*, **68** (1), 87–92, 1968.

[18] **Craig R. R. jr., Kurdila A. J.:** *Fundamentals of Structural Dynamics.* Wiley, 2006.

[19] **Craig R. R. jr., Bampton M. C. C.:** Coupling of substructures for dynamic analysis. *AIAA journal*, **6** (7), 1968.

[20] **Crisfield M. A., Jelenic G.:** Objectivity of strain measures in the geometrically exact three-dimensional beam theory and its finite element implementation. Proceedings of the Royal Society London, **455**, 1125–1147, 1999.

[21] **Dichmann D. J., Maddocks J. H.:** An impetus-striction simulation of the dynamics of an elastica. *Journal of nonlinear science*, **6**, 271–292, 1996.

[22] **Dill E. H.:** Kirchhoff's Theory of Rods, *Archives for history of exact sciences*, **44** (1), 1–23, 1992.

[23] **Ebbinghaus H. D.** et al.: *Numbers.* Springer, 1992.

[24] **Eich-Soellner E., Führer C.:** *Numerical methods in multibody dynamics.* Teubner, 1998.

[25] **Hanson A. J.:** *Visualizing quaternions.* Elsevier, 2005.

[26] **Hodges D. H.:** *Nonlinear composite beam theory.* Progress in astronautics and aeronautics, **213**, 2006.

[27] **Hairer E., Lubich C., Roche M.:** *The numerical solutions of differential-algebraic systems by Runge-Kutta methods.* Springer lecture notes in mathematics, **1409**, 1989.

[28] **Hairer E., Noersett S. P., Wanner G.:** *Solving ordinary differential equations I.* Springer, 1993.

[29] **Hairer E., Wanner G.:** *Solving ordinary differential equations II.* Springer, 1996.

[30] **Hairer E., Lubich C., Wanner G.:** *Geometric numerical integration.* Springer, 2002.

[31] **Ibrahimbegović A.:** On finite element implementations of geometrically nonlinear Reissner's beam theory: Three dimensional curved beam elements. *Computer methods in applied mechanics and engineering*, **112**, 11–26, 1995.

[32] **Ibrahimbegović A., Frey F.:** Finite element analysis of linear and nonlinear planar deformations of elastic initially curved beams. *International journal for numerical methods in engineering*, **36**, 3239–3258, 1992.

[33] **Jung P., Leyendecker S., Linn J., Ortiz M.:** A discrete mechanics approach to Cosserat rod theory — Part I: Static equilibria, *International journal for numerical methods in engineering*, in press, DOI: 10.1002/nme.2950. Preprint: *Berichte des ITWM* Nr. **183**, 2010.

[34] **Kuipers J. B.:** *Quaternions and rotation sequences.* Princeton university press, 1999.

[35] **Kehrbaum S., Maddocks J. H.:** *Elastic rods, rigid bodies, quaternions and the last quadrature.* Philosophical transactions of the royal society London A, **355**, 2117–2136, 1997.

[36] **Kirchhoff G.:** Über das Gleichgewicht und die Bewegung eines unendlich dünnen elastischen Stabes, *Journal für die reine und angewandte Mathematik (Crelle)*, **56**, 285–343, 1859.

[37] **Langer J., Singer D. A.:** Lagrangian aspects of the Kirchhoff elastic rod, *SIAM Review*, **38** (4), 605–618, 1996.

[38] **Lang H., Arnold M.:** Numerical aspects in the dynamic simulation of geometrically exact rods. Accepted for publication in *Applied numerical mathematics*. Preprint: *Berichte des ITWM Kaiserslautern*, **179**, 2009.

[39] **Lang H., Linn J.:** Lagrangian field theory in space-time for geometrically exact Cosserat rods. Preprint: *Berichte des ITWM Kaiserslautern*, **150**, 2009.

[40] **Linn J., Stephan T., Carlsson J., Bohlin R.:** Fast simulation of quasistatic cable deformations for Virtual Reality applications, in: L.L. Bonilla et al. (Eds.): *Progress in Industrial Mathematics at ECMI 2006*, 247–253, Springer, 2007. Preprint: *Berichte des ITWM Kaiserslautern*, **143**.

[41] **Linn J., Stephan T.:** Simulation of quasistatic deformations using discrete rod models. *MULTIBODY DYNAMICS 2007, ECCOMAS Thematic Conference*. Eds: C. L. Bottasso, P. Masarati, L. Trainelli, Milano, Italy, 25-28 June 2007. Preprint: *Berichte des ITWM Kaiserslautern*, **144**.

[42] **Love A. E. H.:** *A Treatise on the Mathematical Theory of Elasticity (4^{th} edition).* Cambridge University Press, 1927, reprinted by Dover, 1944.

[43] **Lubich C.:** Integration of stiff mechanical systems by Runge-Kutta methods. *Journal of applied mathematics and physics*, **44**, 1022–1053, 1993.

[44] **Maddocks J. H.:** Stability of nonlinearly elastic rods, *Archive for rational mechanics and analysis*, **85**, 311–354, 1984.

[45] **Marheineke N., Wegener R.:** Fiber Dynamics in Turbulent Flows: General Modeling Framework *SIAM journal on applied mathematics*, **66** (5), 1703–1726, 2006.

[46] **Matthies H., Strang G.:** *The solution of nonlinear finite element equations.* International journal for numerical methods in engineering, **14**, 1613–1626, 1967.

[47] **Richtmyer R. D., Morton K. W.:** *Difference methods for initial value problems.* Interscience publishers, New York, 1967.

[48] **Nizette M., Goriely A.:** Towards a classification of Euler–Kirchhoff filaments, *Journal of mathematical physics*, **40** (6), 2830–2866, 1999.

[49] **Petzold L. R.:** A description of DASSL: A differential algebraic system solver. In: *Scientific computing*, Stepleman R. S. (Ed.), North-Holland, Amsterdam, 1981.

[50] **Rabier P. J., Rheinboldt W. C.:** *Non-holonomic motion of rigid mechanical systems from a DAE viewpoint.* SIAM, 2000.

[51] **Reissner E.:** On one-dimensional large-displacement finite-strain beam theory, *Studies in applied mathematics*, **52**, 87–95, 1973.

[52] **Romero I.:** The interpolation of rotations and its application to finite-element models of geometrically exact rods. *Computational mechanics*, **34**, 121–133, 2004.

[53] **Sander O.:** Geodesic finite elements for Cosserat rods. *International journal for numerical methods in engineering*, **82** (13), 1645–1670, 2009.

[54] **Schiehlen W. O.:** Multibody system dynamics: Roots and perspectives. *Multibody system dynamics*, **1**, 149–188, 1997.

[55] **Schiehlen W., Eberhard P.:** *Technische Dynamik.* Modelle für Regelung und Simulation. Teubner, 2004.

[56] **Schwab A. L., Meijaard P. J.:** How to draw Euler angles and utilize Euler parameters. *Proceedings of IDETC/CIE*, 2008.

[57] **Shabana A. A.:** Flexible multibody dynamics: Review of past and recent developments. *Multibody system dynamics*, **1**, 189–222, 1997.

[58] **Shabana A. A.:** *Dynamics of multibody systems.* Cambridge, 2005.

[59] **Shoemake K.:** Animating rotation with quaternion curves. ACM SIGGRAPH Computer Graphics, **19** (3), 245–254, 1985.

[60] **Simeon B.:** Numerical analysis of flexible multibody dynamics. *Multibody system dynamics*, **6**, 305–325, 2001.

[61] **Simo J. C.:** A finite strain beam formulation. The three dimensional dynamic problem. Part I. *Computer methods in applied mechanics and engineering*, **49**, 55–70, 1985.

[62] **Simo J. C., Vu-Quoc L.:** A three dimensional finite strain rod model. Part II. *Computer methods in applied mechanics and engineering*, **58**, 79–116, 1986.

[63] **Spillmann J., Teschner M.:** *CoRdE. Cosserat rod elements for the dynamic simulation of one-dimensional elastic objects.* Eurographics/ACM SIGGRAPH, 1–10, 2007.

[64] **Zupan E., Maje M., Zupan D.:** The quaternion–based three–dimensional beam theory. *Computer methods in applied mechanics and engineering*, **198**, 3944–3956, 2009.

Published reports of the Fraunhofer ITWM

The PDF-files of the following reports are available under:
www.itwm.fraunhofer.de/de/zentral__berichte/berichte

1. D. Hietel, K. Steiner, J. Struckmeier
A Finite - Volume Particle Method for Compressible Flows
(19 pages, 1998)

2. M. Feldmann, S. Seibold
Damage Diagnosis of Rotors: Application of Hilbert Transform and Multi-Hypothesis Testing
Keywords: Hilbert transform, damage diagnosis, Kalman filtering, non-linear dynamics
(23 pages, 1998)

3. Y. Ben-Haim, S. Seibold
Robust Reliability of Diagnostic Multi-Hypothesis Algorithms: Application to Rotating Machinery
Keywords: Robust reliability, convex models, Kalman filtering, multi-hypothesis diagnosis, rotating machinery, crack diagnosis
(24 pages, 1998)

4. F.-Th. Lentes, N. Siedow
Three-dimensional Radiative Heat Transfer in Glass Cooling Processes
(23 pages, 1998)

5. A. Klar, R. Wegener
A hierarchy of models for multilane vehicular traffic
Part I: Modeling
(23 pages, 1998)

Part II: Numerical and stochastic investigations
(17 pages, 1998)

6. A. Klar, N. Siedow
Boundary Layers and Domain Decomposition for Radiative Heat Transfer and Diffusion Equations: Applications to Glass Manufacturing Processes
(24 pages, 1998)

7. I. Choquet
Heterogeneous catalysis modelling and numerical simulation in rarified gas flows Part I: Coverage locally at equilibrium
(24 pages, 1998)

8. J. Ohser, B. Steinbach, C. Lang
Efficient Texture Analysis of Binary Images
(17 pages, 1998)

9. J. Orlik
Homogenization for viscoelasticity of the integral type with aging and shrinkage
(20 pages, 1998)

10. J. Mohring
Helmholtz Resonators with Large Aperture
(21 pages, 1998)

11. H. W. Hamacher, A. Schöbel
On Center Cycles in Grid Graphs
(15 pages, 1998)

12. H. W. Hamacher, K.-H. Küfer
Inverse radiation therapy planning - a multiple objective optimisation approach
(14 pages, 1999)

13. C. Lang, J. Ohser, R. Hilfer
On the Analysis of Spatial Binary Images
(20 pages, 1999)

14. M. Junk
On the Construction of Discrete Equilibrium Distributions for Kinetic Schemes
(24 pages, 1999)

15. M. Junk, S. V. Raghurame Rao
A new discrete velocity method for Navier-Stokes equations
(20 pages, 1999)

16. H. Neunzert
Mathematics as a Key to Key Technologies
(39 pages, 1999)

17. J. Ohser, K. Sandau
Considerations about the Estimation of the Size Distribution in Wicksell's Corpuscle Problem
(18 pages, 1999)

18. E. Carrizosa, H. W. Hamacher, R. Klein, S. Nickel
Solving nonconvex planar location problems by finite dominating sets
Keywords: Continuous Location, Polyhedral Gauges, Finite Dominating Sets, Approximation, Sandwich Algorithm, Greedy Algorithm
(19 pages, 2000)

19. A. Becker
A Review on Image Distortion Measures
Keywords: Distortion measure, human visual system
(26 pages, 2000)

20. H. W. Hamacher, M. Labbé, S. Nickel, T. Sonneborn
Polyhedral Properties of the Uncapacitated Multiple Allocation Hub Location Problem
Keywords: integer programming, hub location, facility location, valid inequalities, facets, branch and cut
(21 pages, 2000)

21. H. W. Hamacher, A. Schöbel
Design of Zone Tariff Systems in Public Transportation
(30 pages, 2001)

22. D. Hietel, M. Junk, R. Keck, D. Teleaga
The Finite-Volume-Particle Method for Conservation Laws
(16 pages, 2001)

23. T. Bender, H. Hennes, J. Kalcsics, M. T. Melo, S. Nickel
Location Software and Interface with GIS and Supply Chain Management
Keywords: facility location, software development, geographical information systems, supply chain management
(48 pages, 2001)

24. H. W. Hamacher, S. A. Tjandra
Mathematical Modelling of Evacuation Problems: A State of Art
(44 pages, 2001)

25. J. Kuhnert, S. Tiwari
Grid free method for solving the Poisson equation
Keywords: Poisson equation, Least squares method, Grid free method
(19 pages, 2001)

26. T. Götz, H. Rave, D. Reinel-Bitzer, K. Steiner, H. Tiemeier
Simulation of the fiber spinning process
Keywords: Melt spinning, fiber model, Lattice Boltzmann, CFD
(19 pages, 2001)

27. A. Zemitis
On interaction of a liquid film with an obstacle
Keywords: impinging jets, liquid film, models, numerical solution, shape
(22 pages, 2001)

28. I. Ginzburg, K. Steiner
Free surface lattice-Boltzmann method to model the filling of expanding cavities by Bingham Fluids
Keywords: Generalized LBE, free-surface phenomena, interface boundary conditions, filling processes, Bingham viscoplastic model, regularized models
(22 pages, 2001)

29. H. Neunzert
»Denn nichts ist für den Menschen als Menschen etwas wert, was er nicht mit Leidenschaft tun kann«
Vortrag anlässlich der Verleihung des Akademiepreises des Landes Rheinland-Pfalz am 21.11.2001
Keywords: Lehre, Forschung, angewandte Mathematik, Mehrskalenanalyse, Strömungsmechanik
(18 pages, 2001)

30. J. Kuhnert, S. Tiwari
Finite pointset method based on the projection method for simulations of the incompressible Navier-Stokes equations
Keywords: Incompressible Navier-Stokes equations, Meshfree method, Projection method, Particle scheme, Least squares approximation
AMS subject classification: 76D05, 76M28
(25 pages, 2001)

31. R. Korn, M. Krekel
Optimal Portfolios with Fixed Consumption or Income Streams
Keywords: Portfolio optimisation, stochastic control, HJB equation, discretisation of control problems
(23 pages, 2002)

32. M. Krekel
Optimal portfolios with a loan dependent credit spread
Keywords: Portfolio optimisation, stochastic control, HJB equation, credit spread, log utility, power utility, non-linear wealth dynamics
(25 pages, 2002)

33. J. Ohser, W. Nagel, K. Schladitz
The Euler number of discretized sets – on the choice of adjacency in homogeneous lattices
Keywords: image analysis, Euler number, neighborhod relationships, cuboidal lattice
(32 pages, 2002)

34. I. Ginzburg, K. Steiner
Lattice Boltzmann Model for Free-Surface flow and Its Application to Filling Process in Casting
Keywords: Lattice Boltzmann models; free-surface phenomena; interface boundary conditions; filling processes; injection molding; volume of fluid method; interface boundary conditions; advection-schemes; upwind-schemes
(54 pages, 2002)

35. M. Günther, A. Klar, T. Materne, R. Wegener
Multivalued fundamental diagrams and stop and go waves for continuum traffic equations
Keywords: traffic flow, macroscopic equations, kinetic derivation, multivalued fundamental diagram, stop and go waves, phase transitions
(25 pages, 2002)

36. S. Feldmann, P. Lang, D. Prätzel-Wolters
Parameter influence on the zeros of network determinants
Keywords: Networks, Equicofactor matrix polynomials, Realization theory, Matrix perturbation theory
(30 pages, 2002)

37. K. Koch, J. Ohser, K. Schladitz
Spectral theory for random closed sets and estimating the covariance via frequency space
Keywords: Random set, Bartlett spectrum, fast Fourier transform, power spectrum
(28 pages, 2002)

38. D. d'Humières, I. Ginzburg
Multi-reflection boundary conditions for lattice Boltzmann models
Keywords: lattice Boltzmann equation, boudary condistions, bounce-back rule, Navier-Stokes equation
(72 pages, 2002)

39. R. Korn
Elementare Finanzmathematik
Keywords: Finanzmathematik, Aktien, Optionen, Portfolio-Optimierung, Börse, Lehrerweiterbildung, Mathematikunterricht
(98 pages, 2002)

40. J. Kallrath, M. C. Müller, S. Nickel
Batch Presorting Problems: Models and Complexity Results
Keywords: Complexity theory, Integer programming, Assigment, Logistics
(19 pages, 2002)

41. J. Linn
On the frame-invariant description of the phase space of the Folgar-Tucker equation
Key words: fiber orientation, Folgar-Tucker equation, injection molding
(5 pages, 2003)

42. T. Hanne, S. Nickel
A Multi-Objective Evolutionary Algorithm for Scheduling and Inspection Planning in Software Development Projects
Key words: multiple objective programming, project management and scheduling, software development, evolutionary algorithms, efficient set
(29 pages, 2003)

43. T. Bortfeld , K.-H. Küfer, M. Monz, A. Scherrer, C. Thieke, H. Trinkaus
Intensity-Modulated Radiotherapy - A Large Scale Multi-Criteria Programming Problem
Keywords: multiple criteria optimization, representative systems of Pareto solutions, adaptive triangulation, clustering and disaggregation techniques, visualization of Pareto solutions, medical physics, external beam radiotherapy planning, intensity modulated radiotherapy
(31 pages, 2003)

44. T. Halfmann, T. Wichmann
Overview of Symbolic Methods in Industrial Analog Circuit Design
Keywords: CAD, automated analog circuit design, symbolic analysis, computer algebra, behavioral modeling, system simulation, circuit sizing, macro modeling, differential-algebraic equations, index
(17 pages, 2003)

45. S. E. Mikhailov, J. Orlik
Asymptotic Homogenisation in Strength and Fatigue Durability Analysis of Composites
Keywords: multiscale structures, asymptotic homogenization, strength, fatigue, singularity, non-local conditions
(14 pages, 2003)

46. P. Domínguez-Marín, P. Hansen, N. Mladenovic , S. Nickel
Heuristic Procedures for Solving the Discrete Ordered Median Problem
Keywords: genetic algorithms, variable neighborhood search, discrete facility location
(31 pages, 2003)

47. N. Boland, P. Domínguez-Marín, S. Nickel, J. Puerto
Exact Procedures for Solving the Discrete Ordered Median Problem
Keywords: discrete location, Integer programming
(41 pages, 2003)

48. S. Feldmann, P. Lang
Padé-like reduction of stable discrete linear systems preserving their stability
Keywords: Discrete linear systems, model reduction, stability, Hankel matrix, Stein equation
(16 pages, 2003)

49. J. Kallrath, S. Nickel
A Polynomial Case of the Batch Presorting Problem
Keywords: batch presorting problem, online optimization, competetive analysis, polynomial algorithms, logistics
(17 pages, 2003)

50. T. Hanne, H. L. Trinkaus
knowCube for MCDM – Visual and Interactive Support for Multicriteria Decision Making
Key words: Multicriteria decision making, knowledge management, decision support systems, visual interfaces, interactive navigation, real-life applications.
(26 pages, 2003)

51. O. Iliev, V. Laptev
On Numerical Simulation of Flow Through Oil Filters
Keywords: oil filters, coupled flow in plain and porous media, Navier-Stokes, Brinkman, numerical simulation
(8 pages, 2003)

52. W. Dörfler, O. Iliev, D. Stoyanov, D. Vassileva
On a Multigrid Adaptive Refinement Solver for Saturated Non-Newtonian Flow in Porous Media
Keywords: Nonlinear multigrid, adaptive refinement, non-Newtonian flow in porous media
(17 pages, 2003)

53. S. Kruse
On the Pricing of Forward Starting Options under Stochastic Volatility
Keywords: Option pricing, forward starting options, Heston model, stochastic volatility, cliquet options
(11 pages, 2003)

54. O. Iliev, D. Stoyanov
Multigrid – adaptive local refinement solver for incompressible flows
Keywords: Navier-Stokes equations, incompressible flow, projection-type splitting, SIMPLE, multigrid methods, adaptive local refinement, lid-driven flow in a cavity
(37 pages, 2003)

55. V. Starikovicius
The multiphase flow and heat transfer in porous media
Keywords: Two-phase flow in porous media, various formulations, global pressure, multiphase mixture model, numerical simulation
(30 pages, 2003)

56. P. Lang, A. Sarishvili, A. Wirsen
Blocked neural networks for knowledge extraction in the software development process
Keywords: Blocked Neural Networks, Nonlinear Regression, Knowledge Extraction, Code Inspection
(21 pages, 2003)

57. H. Knaf, P. Lang, S. Zeiser
Diagnosis aiding in Regulation Thermography using Fuzzy Logic
Keywords: fuzzy logic,knowledge representation, expert system
(22 pages, 2003)

58. M. T. Melo, S. Nickel, F. Saldanha da Gama
Largescale models for dynamic multicommodity capacitated facility location
Keywords: supply chain management, strategic planning, dynamic location, modeling
(40 pages, 2003)

59. J. Orlik
Homogenization for contact problems with periodically rough surfaces
Keywords: asymptotic homogenization, contact problems
(28 pages, 2004)

60. A. Scherrer, K.-H. Küfer, M. Monz, F. Alonso, T. Bortfeld
IMRT planning on adaptive volume structures – a significant advance of computational complexity
Keywords: Intensity-modulated radiation therapy (IMRT), inverse treatment planning, adaptive volume structures, hierarchical clustering, local refinement, adaptive clustering, convex programming, mesh generation, multi-grid methods
(24 pages, 2004)

61. D. Kehrwald
Parallel lattice Boltzmann simulation of complex flows
Keywords: Lattice Boltzmann methods, parallel computing, microstructure simulation, virtual material design, pseudo-plastic fluids, liquid composite moulding
(12 pages, 2004)

62. O. Iliev, J. Linn, M. Moog, D. Niedziela, V. Starikovicius
On the Performance of Certain Iterative Solvers for Coupled Systems Arising in Discretization of Non-Newtonian Flow Equations

Keywords: Performance of iterative solvers, Preconditioners, Non-Newtonian flow
(17 pages, 2004)

63. R. Ciegis, O. Iliev, S. Rief, K. Steiner
On Modelling and Simulation of Different Regimes for Liquid Polymer Moulding
Keywords: Liquid Polymer Moulding, Modelling, Simulation, Infiltration, Front Propagation, non-Newtonian flow in porous media
(43 pages, 2004)

64. T. Hanne, H. Neu
Simulating Human Resources in Software Development Processes
Keywords: Human resource modeling, software process, productivity, human factors, learning curve
(14 pages, 2004)

65. O. Iliev, A. Mikelic, P. Popov
Fluid structure interaction problems in deformable porous media: Toward permeability of deformable porous media
Keywords: fluid-structure interaction, deformable porous media, upscaling, linear elasticity, stokes, finite elements
(28 pages, 2004)

66. F. Gaspar, O. Iliev, F. Lisbona, A. Naumovich, P. Vabishchevich
On numerical solution of 1-D poroelasticity equations in a multilayered domain
Keywords: poroelasticity, multilayered material, finite volume discretization, MAC type grid
(41 pages, 2004)

67. J. Ohser, K. Schladitz, K. Koch, M. Nöthe
Diffraction by image processing and its application in materials science
Keywords: porous microstructure, image analysis, random set, fast Fourier transform, power spectrum, Bartlett spectrum
(13 pages, 2004)

68. H. Neunzert
Mathematics as a Technology: Challenges for the next 10 Years
Keywords: applied mathematics, technology, modelling, simulation, visualization, optimization, glass processing, spinning processes, fiber-fluid interaction, trubulence effects, topological optimization, multicriteria optimization, Uncertainty and Risk, financial mathematics, Malliavin calculus, Monte-Carlo methods, virtual material design, filtration, bio-informatics, system biology
(29 pages, 2004)

69. R. Ewing, O. Iliev, R. Lazarov, A. Naumovich
On convergence of certain finite difference discretizations for 1D poroelasticity interface problems
Keywords: poroelasticity, multilayered material, finite volume discretizations, MAC type grid, error estimates
(26 pages,2004)

70. W. Dörfler, O. Iliev, D. Stoyanov, D. Vassileva
On Efficient Simulation of Non-Newtonian Flow in Saturated Porous Media with a Multigrid Adaptive Refinement Solver
Keywords: Nonlinear multigrid, adaptive renement, non-Newtonian in porous media
(25 pages, 2004)

71. J. Kalcsics, S. Nickel, M. Schröder
Towards a Unified Territory Design Approach – Applications, Algorithms and GIS Integration
Keywords: territory desgin, political districting, sales territory alignment, optimization algorithms, Geographical Information Systems
(40 pages, 2005)

72. K. Schladitz, S. Peters, D. Reinel-Bitzer, A. Wiegmann, J. Ohser
Design of acoustic trim based on geometric modeling and flow simulation for non-woven
Keywords: random system of fibers, Poisson line process, flow resistivity, acoustic absorption, Lattice-Boltzmann method, non-woven
(21 pages, 2005)

73. V. Rutka, A. Wiegmann
Explicit Jump Immersed Interface Method for virtual material design of the effective elastic moduli of composite materials
Keywords: virtual material design, explicit jump immersed interface method, effective elastic moduli, composite materials
(22 pages, 2005)

74. T. Hanne
Eine Übersicht zum Scheduling von Baustellen
Keywords: Projektplanung, Scheduling, Bauplanung, Bauindustrie
(32 pages, 2005)

75. J. Linn
The Folgar-Tucker Model as a Differetial Algebraic System for Fiber Orientation Calculation
Keywords: fiber orientation, Folgar–Tucker model, invariants, algebraic constraints, phase space, trace stability
(15 pages, 2005)

76. M. Speckert, K. Dreßler, H. Mauch, A. Lion, G. J. Wierda
Simulation eines neuartigen Prüfsystems für Achserprobungen durch MKS-Modellierung einschließlich Regelung
Keywords: virtual test rig, suspension testing, multibody simulation, modeling hexapod test rig, optimization of test rig configuration
(20 pages, 2005)

77. K.-H. Küfer, M. Monz, A. Scherrer, P. Süss, F. Alonso, A. S. A. Sultan, Th. Bortfeld, D. Craft, Chr. Thieke
Multicriteria optimization in intensity modulated radiotherapy planning
Keywords: multicriteria optimization, extreme solutions, real-time decision making, adaptive approximation schemes, clustering methods, IMRT planning, reverse engineering
(51 pages, 2005)

78. S. Amstutz, H. Andrä
A new algorithm for topology optimization using a level-set method
Keywords: shape optimization, topology optimization, topological sensitivity, level-set
(22 pages, 2005)

79. N. Ettrich
Generation of surface elevation models for urban drainage simulation
Keywords: Flooding, simulation, urban elevation models, laser scanning
(22 pages, 2005)

80. H. Andrä, J. Linn, I. Matei, I. Shklyar, K. Steiner, E. Teichmann
OPTCAST – Entwicklung adäquater Strukturoptimierungsverfahren für Gießereien Technischer Bericht (KURZFASSUNG)
Keywords: Topologieoptimierung, Level-Set-Methode, Gießprozesssimulation, Gießtechnische Restriktionen, CAE-Kette zur Strukturoptimierung
(77 pages, 2005)

81. N. Marheineke, R. Wegener
Fiber Dynamics in Turbulent Flows Part I: General Modeling Framework
Keywords: fiber-fluid interaction; Cosserat rod; turbulence modeling; Kolmogorov's energy spectrum; double-velocity correlations; differentiable Gaussian fields
(20 pages, 2005)

Part II: Specific Taylor Drag
Keywords: flexible fibers; k-ε turbulence model; fiber-turbulence interaction scales; air drag; random Gaussian aerodynamic force; white noise; stochastic differential equations; ARMA process
(18 pages, 2005)

82. C. H. Lampert, O. Wirjadi
An Optimal Non-Orthogonal Separation of the Anisotropic Gaussian Convolution Filter
Keywords: Anisotropic Gaussian filter, linear filtering, orientation space, nD image processing, separable filters
(25 pages, 2005)

83. H. Andrä, D. Stoyanov
Error indicators in the parallel finite element solver for linear elasticity DDFEM
Keywords: linear elasticity, finite element method, hierarchical shape functions, domain decom-position, parallel implementation, a posteriori error estimates
(21 pages, 2006)

84. M. Schröder, I. Solchenbach
Optimization of Transfer Quality in Regional Public Transit
Keywords: public transit, transfer quality, quadratic assignment problem
(16 pages, 2006)

85. A. Naumovich, F. J. Gaspar
On a multigrid solver for the three-dimensional Biot poroelasticity system in multilayered domains
Keywords: poroelasticity, interface problem, multigrid, operator-dependent prolongation
(11 pages, 2006)

86. S. Panda, R. Wegener, N. Marheineke
Slender Body Theory for the Dynamics of Curved Viscous Fibers
Keywords: curved viscous fibers; fluid dynamics; Navier-Stokes equations; free boundary value problem; asymptotic expansions; slender body theory
(14 pages, 2006)

87. E. Ivanov, H. Andrä, A. Kudryavtsev
Domain Decomposition Approach for Automatic Parallel Generation of Tetrahedral Grids
Key words: Grid Generation, Unstructured Grid, Delaunay Triangulation, Parallel Programming, Domain Decomposition, Load Balancing
(18 pages, 2006)

88. S. Tiwari, S. Antonov, D. Hietel, J. Kuhnert, R. Wegener
A Meshfree Method for Simulations of Interactions between Fluids and Flexible Structures
Key words: Meshfree Method, FPM, Fluid Structure Interaction, Sheet of Paper, Dynamical Coupling
(16 pages, 2006)

89. R. Ciegis , O. Iliev, V. Starikovicius, K. Steiner
Numerical Algorithms for Solving Problems of Multiphase Flows in Porous Media
Keywords: nonlinear algorithms, finite-volume method, software tools, porous media, flows
(16 pages, 2006)

90. D. Niedziela, O. Iliev, A. Latz
On 3D Numerical Simulations of Viscoelastic Fluids
Keywords: non-Newtonian fluids, anisotropic viscosity, integral constitutive equation
(18 pages, 2006)

91. A. Winterfeld
Application of general semi-infinite Programming to Lapidary Cutting Problems
Keywords: large scale optimization, nonlinear programming, general semi-infinite optimization, design centering, clustering
(26 pages, 2006)

92. J. Orlik, A. Ostrovska
Space-Time Finite Element Approximation and Numerical Solution of Hereditary Linear Viscoelasticity Problems
Keywords: hereditary viscoelasticity; kern approximation by interpolation; space-time finite element approximation, stability and a priori estimate
(24 pages, 2006)

93. V. Rutka, A. Wiegmann, H. Andrä
EJIIM for Calculation of effective Elastic Moduli in 3D Linear Elasticity
Keywords: Elliptic PDE, linear elasticity, irregular domain, finite differences, fast solvers, effective elastic moduli
(24 pages, 2006)

94. A. Wiegmann, A. Zemitis
EJ-HEAT: A Fast Explicit Jump Harmonic Averaging Solver for the Effective Heat Conductivity of Composite Materials
Keywords: Stationary heat equation, effective thermal conductivity, explicit jump, discontinuous coefficients, virtual material design, microstructure simulation, EJ-HEAT
(21 pages, 2006)

95. A. Naumovich
On a finite volume discretization of the three-dimensional Biot poroelasticity system in multilayered domains
Keywords: Biot poroelasticity system, interface problems, finite volume discretization, finite difference method
(21 pages, 2006)

96. M. Krekel, J. Wenzel
A unified approach to Credit Default Swaption and Constant Maturity Credit Default Swap valuation
Keywords: LIBOR market model, credit risk, Credit Default Swaption, Constant Maturity Credit Default Swap-method
(43 pages, 2006)

97. A. Dreyer
Interval Methods for Analog Circiuts
Keywords: interval arithmetic, analog circuits, tolerance analysis, parametric linear systems, frequency response, symbolic analysis, CAD, computer algebra
(36 pages, 2006)

98. N. Weigel, S. Weihe, G. Bitsch, K. Dreßler
Usage of Simulation for Design and Optimization of Testing
Keywords: Vehicle test rigs, MBS, control, hydraulics, testing philosophy
(14 pages, 2006)

99. H. Lang, G. Bitsch, K. Dreßler, M. Speckert
Comparison of the solutions of the elastic and elastoplastic boundary value problems
Keywords: Elastic BVP, elastoplastic BVP, variational inequalities, rate-independency, hysteresis, linear kinematic hardening, stop- and play-operator
(21 pages, 2006)

100. M. Speckert, K. Dreßler, H. Mauch
MBS Simulation of a hexapod based suspension test rig
Keywords: Test rig, MBS simulation, suspension, hydraulics, controlling, design optimization
(12 pages, 2006)

101. S. Azizi Sultan, K.-H. Küfer
A dynamic algorithm for beam orientations in multicriteria IMRT planning
Keywords: radiotherapy planning, beam orientation optimization, dynamic approach, evolutionary algorithm, global optimization
(14 pages, 2006)

102. T. Götz, A. Klar, N. Marheineke, R. Wegener
A Stochastic Model for the Fiber Lay-down Process in the Nonwoven Production
Keywords: fiber dynamics, stochastic Hamiltonian system, stochastic averaging
(17 pages, 2006)

103. Ph. Süss, K.-H. Küfer
Balancing control and simplicity: a variable aggregation method in intensity modulated radiation therapy planning
Keywords: IMRT planning, variable aggregation, clustering methods
(22 pages, 2006)

104. A. Beaudry, G. Laporte, T. Melo, S. Nickel
Dynamic transportation of patients in hospitals
Keywords: in-house hospital transportation, dial-a-ride, dynamic mode, tabu search
(37 pages, 2006)

105. Th. Hanne
Applying multiobjective evolutionary algorithms in industrial projects
Keywords: multiobjective evolutionary algorithms, discrete optimization, continuous optimization, electronic circuit design, semi-infinite programming, scheduling
(18 pages, 2006)

106. J. Franke, S. Halim
Wild bootstrap tests for comparing signals and images
Keywords: wild bootstrap test, texture classification, textile quality control, defect detection, kernel estimate, nonparametric regression
(13 pages, 2007)

107. Z. Drezner, S. Nickel
Solving the ordered one-median problem in the plane
Keywords: planar location, global optimization, ordered median, big triangle small triangle method, bounds, numerical experiments
(21 pages, 2007)

108. Th. Götz, A. Klar, A. Unterreiter, R. Wegener
Numerical evidance for the non-existing of solutions of the equations desribing rotational fiber spinning
Keywords: rotational fiber spinning, viscous fibers, boundary value problem, existence of solutions
(11 pages, 2007)

109. Ph. Süss, K.-H. Küfer
Smooth intensity maps and the Bortfeld-Boyer sequencer
Keywords: probabilistic analysis, intensity modulated radiotherapy treatment (IMRT), IMRT plan application, step-and-shoot sequencing
(8 pages, 2007)

110. E. Ivanov, O. Gluchshenko, H. Andrä, A. Kudryavtsev
Parallel software tool for decomposing and meshing of 3d structures
Keywords: a-priori domain decomposition, unstructured grid, Delaunay mesh generation
(14 pages, 2007)

111. O. Iliev, R. Lazarov, J. Willems
Numerical study of two-grid preconditioners for 1d elliptic problems with highly oscillating discontinuous coefficients
Keywords: two-grid algorithm, oscillating coefficients, preconditioner
(20 pages, 2007)

112. L. Bonilla, T. Götz, A. Klar, N. Marheineke, R. Wegener
Hydrodynamic limit of the Fokker-Planck-equation describing fiber lay-down processes
Keywords: stochastic dierential equations, Fokker-Planck equation, asymptotic expansion, Ornstein-Uhlenbeck process
(17 pages, 2007)

113. S. Rief
Modeling and simulation of the pressing section of a paper machine
Keywords: paper machine, computational fluid dynamics, porous media
(41 pages, 2007)

114. R. Ciegis, O. Iliev, Z. Lakdawala
On parallel numerical algorithms for simulating industrial filtration problems
Keywords: Navier-Stokes-Brinkmann equations, finite volume discretization method, SIMPLE, parallel computing, data decomposition method
(24 pages, 2007)

115. N. Marheineke, R. Wegener
Dynamics of curved viscous fibers with surface tension
Keywords: Slender body theory, curved viscous bers with surface tension, free boundary value problem
(25 pages, 2007)

116. S. Feth, J. Franke, M. Speckert
Resampling-Methoden zur mse-Korrektur und Anwendungen in der Betriebsfestigkeit
Keywords: Weibull, Bootstrap, Maximum-Likelihood, Betriebsfestigkeit
(16 pages, 2007)

117. H. Knaf
Kernel Fisher discriminant functions – a concise and rigorous introduction
Keywords: wild bootstrap test, texture classification, textile quality control, defect detection, kernel estimate, nonparametric regression
(30 pages, 2007)

118. O. Iliev, I. Rybak
On numerical upscaling for flows in heterogeneous porous media

Keywords: numerical upscaling, heterogeneous porous media, single phase flow, Darcy's law, multiscale problem, effective permeability, multipoint flux approximation, anisotropy
(17 pages, 2007)

119. O. Iliev, I. Rybak
On approximation property of multipoint flux approximation method
Keywords: Multipoint flux approximation, finite volume method, elliptic equation, discontinuous tensor coefficients, anisotropy
(15 pages, 2007)

120. O. Iliev, I. Rybak, J. Willems
On upscaling heat conductivity for a class of industrial problems
Keywords: Multiscale problems, effective heat conductivity, numerical upscaling, domain decomposition
(21 pages, 2007)

121. R. Ewing, O. Iliev, R. Lazarov, I. Rybak
On two-level preconditioners for flow in porous media
Keywords: Multiscale problem, Darcy's law, single phase flow, anisotropic heterogeneous porous media, numerical upscaling, multigrid, domain decomposition, efficient preconditioner
(18 pages, 2007)

122. M. Brickenstein, A. Dreyer
POLYBORI: A Gröbner basis framework for Boolean polynomials
Keywords: Gröbner basis, formal verification, Boolean polynomials, algebraic cryptoanalysis, satisfiability
(23 pages, 2007)

123. O. Wirjadi
Survey of 3d image segmentation methods
Keywords: image processing, 3d, image segmentation, binarization
(20 pages, 2007)

124. S. Zeytun, A. Gupta
A Comparative Study of the Vasicek and the CIR Model of the Short Rate
Keywords: interest rates, Vasicek model, CIR-model, calibration, parameter estimation
(17 pages, 2007)

125. G. Hanselmann, A. Sarishvili
Heterogeneous redundancy in software quality prediction using a hybrid Bayesian approach
Keywords: reliability prediction, fault prediction, non-homogeneous poisson process, Bayesian model averaging
(17 pages, 2007)

126. V. Maag, M. Berger, A. Winterfeld, K.-H. Küfer
A novel non-linear approach to minimal area rectangular packing
Keywords: rectangular packing, non-overlapping constraints, non-linear optimization, regularization, relaxation
(18 pages, 2007)

127. M. Monz, K.-H. Küfer, T. Bortfeld, C. Thieke
Pareto navigation – systematic multi-criteria-based IMRT treatment plan determination
Keywords: convex, interactive multi-objective optimization, intensity modulated radiotherapy planning
(15 pages, 2007)

128. M. Krause, A. Scherrer
On the role of modeling parameters in IMRT plan optimization
Keywords: intensity-modulated radiotherapy (IMRT), inverse IMRT planning, convex optimization, sensitivity analysis, elasticity, modeling parameters, equivalent uniform dose (EUD)
(18 pages, 2007)

129. A. Wiegmann
Computation of the permeability of porous materials from their microstructure by FFF-Stokes
Keywords: permeability, numerical homogenization, fast Stokes solver
(24 pages, 2007)

130. T. Melo, S. Nickel, F. Saldanha da Gama
Facility Location and Supply Chain Management – A comprehensive review
Keywords: facility location, supply chain management, network design
(54 pages, 2007)

131. T. Hanne, T. Melo, S. Nickel
Bringing robustness to patient flow management through optimized patient transports in hospitals
Keywords: Dial-a-Ride problem, online problem, case study, tabu search, hospital logistics
(23 pages, 2007)

132. R. Ewing, O. Iliev, R. Lazarov, I. Rybak, J. Willems
An efficient approach for upscaling properties of composite materials with high contrast of coefficients
Keywords: effective heat conductivity, permeability of fractured porous media, numerical upscaling, fibrous insulation materials, metal foams
(16 pages, 2008)

133. S. Gelareh, S. Nickel
New approaches to hub location problems in public transport planning
Keywords: integer programming, hub location, transportation, decomposition, heuristic
(25 pages, 2008)

134. G. Thömmes, J. Becker, M. Junk, A. K. Vaikuntam, D. Kehrwald, A. Klar, K. Steiner, A. Wiegmann
A Lattice Boltzmann Method for immiscible multiphase flow simulations using the Level Set Method
Keywords: Lattice Boltzmann method, Level Set method, free surface, multiphase flow
(28 pages, 2008)

135. J. Orlik
Homogenization in elasto-plasticity
Keywords: multiscale structures, asymptotic homogenization, nonlinear energy
(40 pages, 2008)

136. J. Almquist, H. Schmidt, P. Lang, J. Deitmer, M. Jirstrand, D. Prätzel-Wolters, H. Becker
Determination of interaction between MCT1 and CAII via a mathematical and physiological approach
Keywords: mathematical modeling; model reduction; electrophysiology; pH-sensitive microelectrodes; proton antenna
(20 pages, 2008)

137. E. Savenkov, H. Andrä, O. Iliev
An analysis of one regularization approach for solution of pure Neumann problem
Keywords: pure Neumann problem, elasticity, regularization, finite element method, condition number
(27 pages, 2008)

138. O. Berman, J. Kalcsics, D. Krass, S. Nickel
The ordered gradual covering location problem on a network
Keywords: gradual covering, ordered median function, network location
(32 pages, 2008)

139. S. Gelareh, S. Nickel
Multi-period public transport design: A novel model and solution approaches
Keywords: Integer programming, hub location, public transport, multi-period planning, heuristics
(31 pages, 2008)

140. T. Melo, S. Nickel, F. Saldanha-da-Gama
Network design decisions in supply chain planning
Keywords: supply chain design, integer programming models, location models, heuristics
(20 pages, 2008)

141. C. Lautensack, A. Särkkä, J. Freitag, K. Schladitz
Anisotropy analysis of pressed point processes
Keywords: estimation of compression, isotropy test, nearest neighbour distance, orientation analysis, polar ice, Ripley's K function
(35 pages, 2008)

142. O. Iliev, R. Lazarov, J. Willems
A Graph-Laplacian approach for calculating the effective thermal conductivity of complicated fiber geometries
Keywords: graph laplacian, effective heat conductivity, numerical upscaling, fibrous materials
(14 pages, 2008)

143. J. Linn, T. Stephan, J. Carlsson, R. Bohlin
Fast simulation of quasistatic rod deformations for VR applications
Keywords: quasistatic deformations, geometrically exact rod models, variational formulation, energy minimization, finite differences, nonlinear conjugate gradients
(7 pages, 2008)

144. J. Linn, T. Stephan
Simulation of quasistatic deformations using discrete rod models
Keywords: quasistatic deformations, geometrically exact rod models, variational formulation, energy minimization, finite differences, nonlinear conjugate gradients
(9 pages, 2008)

145. J. Marburger, N. Marheineke, R. Pinnau
Adjoint based optimal control using mesh-less discretizations
Keywords: Mesh-less methods, particle methods, Eulerian-Lagrangian formulation, optimization strategies, adjoint method, hyperbolic equations
(14 pages, 2008

146. S. Desmettre, J. Gould, A. Szimayer
Own-company stockholding and work effort preferences of an unconstrained executive
Keywords: optimal portfolio choice, executive compensation
(33 pages, 2008)

147. M. Berger, M. Schröder, K.-H. Küfer
A constraint programming approach for the two-dimensional rectangular packing problem with orthogonal orientations
Keywords: rectangular packing, orthogonal orientations non-overlapping constraints, constraint propagation
(13 pages, 2008)

148. K. Schladitz, C. Redenbach, T. Sych, M. Godehardt
Microstructural characterisation of open foams using 3d images
Keywords: virtual material design, image analysis, open foams
(30 pages, 2008)

149. E. Fernández, J. Kalcsics, S. Nickel, R. Ríos-Mercado
A novel territory design model arising in the implementation of the WEEE-Directive
Keywords: heuristics, optimization, logistics, recycling
(28 pages, 2008)

150. H. Lang, J. Linn
Lagrangian field theory in space-time for geometrically exact Cosserat rods
Keywords: Cosserat rods, geometrically exact rods, small strain, large deformation, deformable bodies, Lagrangian field theory, variational calculus
(19 pages, 2009)

151. K. Dreßler, M. Speckert, R. Müller, Ch. Weber
Customer loads correlation in truck engineering
Keywords: Customer distribution, safety critical components, quantile estimation, Monte-Carlo methods
(11 pages, 2009)

152. H. Lang, K. Dreßler
An improved multiaxial stress-strain correction model for elastic FE postprocessing
Keywords: Jiang's model of elastoplasticity, stress-strain correction, parameter identification, automatic differentiation, least-squares optimization, Coleman-Li algorithm
(6 pages, 2009)

153. J. Kalcsics, S. Nickel, M. Schröder
A generic geometric approach to territory design and districting
Keywords: Territory design, districting, combinatorial optimization, heuristics, computational geometry
(32 pages, 2009)

154. Th. Fütterer, A. Klar, R. Wegener
An energy conserving numerical scheme for the dynamics of hyperelastic rods
Keywords: Cosserat rod, hyperealstic, energy conservation, finite differences
(16 pages, 2009)

155. A. Wiegmann, L. Cheng, E. Glatt, O. Iliev, S. Rief
Design of pleated filters by computer simulations
Keywords: Solid-gas separation, solid-liquid separation, pleated filter, design, simulation
(21 pages, 2009)

156. A. Klar, N. Marheineke, R. Wegener
Hierarchy of mathematical models for production processes of technical textiles
Keywords: Fiber-fluid interaction, slender-body theory, turbulence modeling, model reduction, stochastic differential equations, Fokker-Planck equation, asymptotic expansions, parameter identification
(21 pages, 2009)

157. E. Glatt, S. Rief, A. Wiegmann, M. Knefel, E. Wegenke
Structure and pressure drop of real and virtual metal wire meshes
Keywords: metal wire mesh, structure simulation, model calibration, CFD simulation, pressure loss
(7 pages, 2009)

158. S. Kruse, M. Müller
Pricing American call options under the assumption of stochastic dividends – An application of the Korn-Rogers model
Keywords: option pricing, American options, dividends, dividend discount model, Black-Scholes model
(22 pages, 2009)

159. H. Lang, J. Linn, M. Arnold
Multibody dynamics simulation of geometrically exact Cosserat rods
Keywords: flexible multibody dynamics, large deformations, finite rotations, constrained mechanical systems, structural dynamics
(20 pages, 2009)

160. P. Jung, S. Leyendecker, J. Linn, M. Ortiz
Discrete Lagrangian mechanics and geometrically exact Cosserat rods
Keywords: special Cosserat rods, Lagrangian mechanics, Noether's theorem, discrete mechanics, frame-indifference, holonomic constraints
(14 pages, 2009)

161. M. Burger, K. Dreßler, A. Marquardt, M. Speckert
Calculating invariant loads for system simulation in vehicle engineering
Keywords: iterative learning control, optimal control theory, differential algebraic equations (DAEs)
(18 pages, 2009)

162. M. Speckert, N. Ruf, K. Dreßler
Undesired drift of multibody models excited by measured accelerations or forces
Keywords: multibody simulation, full vehicle model, force-based simulation, drift due to noise
(19 pages, 2009)

163. A. Streit, K. Dreßler, M. Speckert, J. Lichter, T. Zenner, P. Bach
Anwendung statistischer Methoden zur Erstellung von Nutzungsprofilen für die Auslegung von Mobilbaggern
Keywords: Nutzungsvielfalt, Kundenbeanspruchung, Bemessungsgrundlagen
(13 pages, 2009)

164. I. Correia, S. Nickel, F. Saldanha-da-Gama
The capacitated single-allocation hub location problem revisited: A note on a classical formulation
Keywords: Capacitated Hub Location, MIP formulations
(10 pages, 2009)

165. F. Yaneva, T. Grebe, A. Scherrer
An alternative view on global radiotherapy optimization problems
Keywords: radiotherapy planning, path-connected sublevelsets, modified gradient projection method, improving and feasible directions
(14 pages, 2009)

166. J. I. Serna, M. Monz, K.-H. Küfer, C. Thieke
Trade-off bounds and their effect in multi-criteria IMRT planning
Keywords: trade-off bounds, multi-criteria optimization, IMRT, Pareto surface
(15 pages, 2009)

167. W. Arne, N. Marheineke, A. Meister, R. Wegener
Numerical analysis of Cosserat rod and string models for viscous jets in rotational spinning processes
Keywords: Rotational spinning process, curved viscous fibers, asymptotic Cosserat models, boundary value problem, existence of numerical solutions
(18 pages, 2009)

168. T. Melo, S. Nickel, F. Saldanha-da-Gama
An LP-rounding heuristic to solve a multi-period facility relocation problem
Keywords: supply chain design, heuristic, linear programming, rounding
(37 pages, 2009)

169. I. Correia, S. Nickel, F. Saldanha-da-Gama
Single-allocation hub location problems with capacity choices
Keywords: hub location, capacity decisions, MILP formulations
(27 pages, 2009)

170. S. Acar, K. Natcheva-Acar
A guide on the implementation of the Heath-Jarrow-Morton Two-Factor Gaussian Short Rate Model (HJM-G2++)
Keywords: short rate model, two factor Gaussian, G2++, option pricing, calibration
(30 pages, 2009)

171. A. Szimayer, G. Dimitroff, S. Lorenz
A parsimonious multi-asset Heston model: calibration and derivative pricing
Keywords: Heston model, multi-asset, option pricing, calibration, correlation
(28 pages, 2009)

172. N. Marheineke, R. Wegener
Modeling and validation of a stochastic drag for fibers in turbulent flows
Keywords: fiber-fluid interactions, long slender fibers, turbulence modelling, aerodynamic drag, dimensional analysis, data interpolation, stochastic partial differential algebraic equation, numerical simulations, experimental validations
(19 pages, 2009)

173. S. Nickel, M. Schröder, J. Steeg
Planning for home health care services
Keywords: home health care, route planning, metaheuristics, constraint programming
(23 pages, 2009)

174. G. Dimitroff, A. Szimayer, A. Wagner
Quanto option pricing in the parsimonious Heston model
Keywords: Heston model, multi asset, quanto options, option pricing
(14 pages, 2009) 174. G. Dimitroff, A. Szimayer, A. Wagner

175. S. Herkt, K. Dreßler, R. Pinnau
Model reduction of nonlinear problems in structural mechanics
Keywords: flexible bodies, FEM, nonlinear model reduction, POD
(13 pages, 2009)

176. M. K. Ahmad, S. Didas, J. Iqbal
Using the Sharp Operator for edge detection and nonlinear diffusion
Keywords: maximal function, sharp function,image processing, edge detection, nonlinear diffusion
(17 pages, 2009)

177. M. Speckert, N. Ruf, K. Dreßler, R. Müller, C. Weber, S. Weihe
Ein neuer Ansatz zur Ermittlung von Erprobungslasten für sicherheitsrelevante Bauteile
Keywords: sicherheitsrelevante Bauteile, Kundenbeanspruchung, Festigkeitsverteilung, Ausfallwahrscheinlichkeit, Konfidenz, statistische Unsicherheit, Sicherheitsfaktoren
(16 pages, 2009)

178. J. Jegorovs
Wave based method: new applicability areas
Keywords: Elliptic boundary value problems, inhomogeneous Helmholtz type differential equations in bounded domains, numerical methods, wave based method, uniform B-splines
(10 pages, 2009)

179. H. Lang, M. Arnold
Numerical aspects in the dynamic simulation of geometrically exact rods
Keywords: Kirchhoff and Cosserat rods, geometrically exact rods, deformable bodies, multibody dynamics,artial differential algebraic equations, method of lines, time integration
(21 pages, 2009)

180. H. Lang
Comparison of quaternionic and rotation-free null space formalisms for multibody dynamics
Keywords: Parametrisation of rotations, differential-algebraic equations, multibody dynamics, constrained mechanical systems, Lagrangian mechanics
(40 pages, 2010)

181. S. Nickel, F. Saldanha-da-Gama, H.-P. Ziegler
Stochastic programming approaches for risk aware supply chain network design problems
Keywords: Supply Chain Management, multi-stage stochastic programming, financial decisions, risk
(37 pages, 2010)

182. P. Ruckdeschel, N. Horbenko
Robustness properties of estimators in generalized Pareto Models
Keywords: global robustness, local robustness, finite sample breakdown point, generalized Pareto distribution
(58 pages, 2010)

183. P. Jung, S. Leyendecker, J. Linn, M. Ortiz
A discrete mechanics approach to Cosserat rod theory – Part 1: static equilibria
Keywords: Special Cosserat rods; Lagrangian mechanics; Noether's theorem; discrete mechanics; frame-indifference; holonomic constraints; variational formulation
(35 pages, 2010)

184. R. Eymard, G. Printsypar
A proof of convergence of a finite volume scheme for modified steady Richards' equation describing transport processes in the pressing section of a paper machine
Keywords: flow in porous media, steady Richards' equation, finite volume methods, convergence of approximate solution
(14 pages, 2010)

185. P. Ruckdeschel
Optimally Robust Kalman Filtering
Keywords: robustness, Kalman Filter, innovation outlier, additive outlier
(42 pages, 2010)

186. S. Repke, N. Marheineke, R. Pinnau
On adjoint-based optimization of a free surface Stokes flow
Keywords: film casting process, thin films, free surface Stokes flow, optimal control, Lagrange formalism
(13 pages, 2010)

187. O. Iliev, R. Lazarov, J. Willems
Variational multiscale Finite Element Method for flows in highly porous media
Keywords: numerical upscaling, flow in heterogeneous porous media, Brinkman equations, Darcy's law, subgrid approximation, discontinuous Galerkin mixed FEM
(21 pages, 2010)

188. S. Desmettre, A. Szimayer
Work effort, consumption, and portfolio selection: When the occupational choice matters
Keywords: portfolio choice, work effort, consumption, occupational choice
(34 pages, 2010)

189. O. Iliev, Z. Lakdawala, V. Starikovicius
On a numerical subgrid upscaling algorithm for Stokes-Brinkman equations
Keywords: Stokes-Brinkman equations, subgrid approach, multiscale problems, numerical upscaling
(27 pages, 2010)

190. A. Latz, J. Zausch, O. Iliev
Modeling of species and charge transport in Li-Ion Batteries based on non-equilibrium thermodynamics
Keywords: lithium-ion battery, battery modeling, electrochemical simulation, concentrated electrolyte, ion transport
(8 pages, 2010)

191. P. Popov, Y. Vutov, S. Margenov, O. Iliev
Finite volume discretization of equations describing nonlinear diffusion in Li-Ion batteries
Keywords: nonlinear diffusion, finite volume discretization, Newton method, Li-Ion batteries
(9 pages, 2010)

192. W. Arne, N. Marheineke, R. Wegener
Asymptotic transition from Cosserat rod to string models for curved viscous inertial jets
Keywords: rotational spinning processes; inertial and viscous-inertial fiber regimes; asymptotic limits; slender-body theory; boundary value problems
(23 pages, 2010)

193. L. Engelhardt, M. Burger, G. Bitsch
Real-time simulation of multibody-systems for on-board applications
Keywords: multibody system simulation, real-time simulation, on-board simulation, Rosenbrock methods
(10 pages, 2010)

194. M. Burger, M. Speckert, K. Dreßler
Optimal control methods for the calculation of invariant excitation signals for multibody systems
Keywords: optimal control, optimization, mbs simulation, invariant excitation
(9 pages, 2010)

195. A. Latz, J. Zausch
Thermodynamic consistent transport theory of Li-Ion batteries
Keywords: Li-Ion batteries, nonequilibrium thermodynamics, thermal transport, modeling
(18 pages, 2010)

196. S. Desmettre
Optimal investment for executive stockholders with exponential utility
Keywords: portfolio choice, executive stockholder, work effort, exponential utility
(24 pages, 2010)

197. W. Arne, N. Marheineke, J. Schnebele, R. Wegener
Fluid-fiber-interactions in rotational spinning process of glass wool production
Keywords: Rotational spinning process, viscous thermal jets, fluid-fiber-interactions, two-way coupling, slender-body theory, Cosserat rods, drag models, boundary value problem, continuation method
(20 pages, 2010)

198. A. Klar, J. Maringer, R. Wegener
A 3d model for fiber lay-down in nonwoven production processes
Keywords: fiber dynamics, Fokker-Planck equations, diffusion limits
(15 pages, 2010)

199. Ch. Erlwein, M. Müller
A regime-switching regression model for hedge funds
Keywords: switching regression model, Hedge funds, optimal parameter estimation, filtering
(26 pages, 2011)

200. M. Dalheimer
Power to the people – Das Stromnetz der Zukunft
Keywords: Smart Grid, Stromnetz, Erneuerbare Energien, Demand-Side Management
(27 pages, 2011)

201. D. Stahl, J. Hauth
PF-MPC: Particle Filter-Model Predictive Control
Keywords: Model Predictive Control, Particle Filter, CSTR, Inverted Pendulum, Nonlinear Systems, Sequential Monte Carlo
(40 pages, 2011)

202. G. Dimitroff, J. de Kock
Calibrating and completing the volatility cube in the SABR Model
Keywords: stochastic volatility, SABR, volatility cube, swaption
(12 pages, 2011)

203. J.-P. Kreiss, T. Zangmeister
Quantification of the effectiveness of a safety function in passenger vehicles on the basis of real-world accident data
Keywords: logistic regression, safety function, real-world accident data, statistical modeling
(23 pages, 2011)

204. P. Ruckdeschel, T. Sayer, A. Szimayer
Pricing American options in the Heston model: a close look on incorporating correlation
Keywords: Heston model, American options, moment matching, correlation, tree method
(30 pages, 2011)

205. H. Ackermann, H. Ewe, K.-H. Küfer, M. Schröder
Modeling profit sharing in combinatorial exchanges by network flows
Keywords: Algorithmic game theory, profit sharing, combinatorial exchange, network flows, budget balance, core
(17 pages, 2011)

206. O. Iliev, G. Printsypar, S. Rief
A one-dimensional model of the pressing section of a paper machine including dynamic capillary effects
Keywords: steady modified Richards' equation, finite volume method, dynamic capillary pressure, pressing section of a paper machine
(29 pages, 2011)

207. I. Vecchio, K. Schladitz, M. Godehardt, M. J. Heneka
Geometric characterization of particles in 3d with an application to technical cleanliness
Keywords: intrinsic volumes, isoperimetric shape factors, bounding box, elongation, geodesic distance, technical cleanliness
(21 pages, 2011)

208. M. Burger, K. Dreßler, M. Speckert
Invariant input loads for full vehicle multibody system simulation
Keywords: multibody systems, full-vehicle simulation, optimal control
(8 pages, 2011)

209. H. Lang, J. Linn, M. Arnold
Multibody dynamics simulation of geometrically exact Cosserat rods
Keywords: flexible multibody dynamics, large deformations, finite rotations, constrained mechanical systems, structural dynamics
(28 pages, 2011)

Status quo: November 2011